

## NEURAL NETWORKS FOR MODELING OF ELECTRICAL PARAMETERS AND LOSSES IN ELECTRIC VEHICLE

Master Degree Project in Virtual Product Realization

One year Level 18 ECTS

Spring term 2023

Yo Fujimoto

Supervisors: Richard Senington, Kristian Holmberg

Examiner: Sunith Bandaru

## Abstract

Permanent magnet synchronous machines have various advantages and have showed the most superior performance for Electric Vehicles. However, modeling them is difficult because of their nonlinearity. In order to deal with the complexity, the artificial neural network and machine learning models including k-nearest neighbors, decision tree, random forest, and multiple linear regression with a quadratic model are developed to predict electrical parameters and losses as new prediction approaches for the performance of Volvo Cars' electric vehicles and evaluate their performance.

The test operation data of the Volvo Cars Corporation was used to extract and calculate the input and output data for each prediction model. In order to smooth the effects of each input variable, the input data was normalized. In addition, correlation matrices of normalized inputs were produced, which showed a high correlation between rotor temperature and winding resistance in the electrical parameter prediction dataset. They also demonstrated a strong correlation between the winding temperature and the rotor temperature in the loss prediction dataset.

Grid search with 5-fold cross validation was implemented to optimize hyperparameters of artificial neural network and machine learning models. The artificial neural network models performed the best in MSE and R-squared scores for all the electrical parameters and loss prediction. The results indicate that artificial neural networks are more successful at handling complicated nonlinear relationships like those seen in electrical systems compared with other machine learning algorithms. Compared to other machine learning algorithms like decision trees, k-nearest neighbors, and multiple linear regression with a quadratic model, random forest produced superior results. With the exception of q-axis voltage, the decision tree model outperformed the k-nearest neighbors model in terms of parameter prediction, as measured by MSE and R-squared score. Multiple linear regression with a quadratic model produced the worst results for the electric parameters prediction because the relationship between the input and output was too complex for a **multiple quadratic equation** to deal with. Random forest models performed better than decision tree models because random forest ensemble hundreds of subset of decision trees and averaging the results. The k-nearest neighbors performed worse for almost all electrical parameters anticipation than the decision tree because it simply chooses the closest points and uses the average as the projected outputs so it was challenging to forecast complex nonlinear relationships. However, it is helpful for handling simple relationships and for understanding relationships in data. In terms of loss prediction, the k-nearest neighbors and decision tree produced similar results in MSE and R-squared score for the electric machine loss and the inverter loss. Their prediction results were worse than the multiple linear regression with a quadratic model, but they performed better than the multiple linear regression with a quadratic model, for forecasting the power difference between electromagnetic power and mechanical power.

**Keywords:** Artificial neural network, machine learning, random forest, deep learning, electric vehicle, decision tree, k-nearest neighbors, permanent magnet synchronous machine

## Acknowledgements

I would like to appreciate my supervisor Kristian Holmberg at Volvo Cars Corporation for the opportunity of thesis work and valuable suggestions to improve the quality of the thesis work. Also, I would like to thank Shayan Halder at Volvo Cars for his great support and advice during the thesis work.

I would like appreciate to my supervisor, Richard Senington at the University of Skovde, for his advice and response to any questions. I sincerely gratitude to my examiner Sunith Bandaru at University of Skovde, for all his comments and feedback to improve the thesis project.

Skövde, June 2023

Yo Fujimoto



HÖGSKOLAN  
I SKÖVDE

## Table of Contents

1. Introduction .....	1
1.1 Research problem .....	1
1.2 Aim and objectives .....	2
1.3 Scope and limitations.....	2
2. Theoretical Framework.....	3
2.1 Artificial neural networks .....	3
2.1.1 Feedforward process.....	4
2.1.2 Backpropagation.....	5
2.2 K-nearest neighbors regression .....	5
2.3 Decision tree regression.....	6
2.4 Random forest regression .....	7
2.5 Multiple linear regression with a quadratic model .....	7
2.6 Cross validation .....	8
2.7 Hyperparameter tuning .....	8
3. Literature Review and Related Works .....	10
3.1 Machine Learning.....	10
3.2 Artificial neural network and machine learning for industrial applications .....	10
3.3 Artificial neural network and other machine learning for PMSM parameters and losses prediction.....	12
4. Experimental Methodology .....	14
4.1 Data collection and preparation.....	14
4.1.1 Data for electrical parameter prediction .....	14
4.1.2 Data for loss prediction.....	18
4.2 Develop artificial neural network and machine learning models .....	22
4.2.1 Hyperparameter tuning of artificial neural network .....	23
4.2.2 Hyperparameter tuning of k-nearest neighbors .....	23
4.2.3 Hyperparameter tuning of decision tree .....	23
4.2.4 Hyperparameter tuning of random forest .....	24
4.3 Model evaluation .....	24

5. Results and Discussion .....	26
5.1 Prediction results with default parameter .....	26
5.2 Hyperparameter tuning .....	30
5.2.1 Hyperparameter tuning of artificial neural network .....	30
5.2.2 Hyperparameter tuning of k-nearest neighbors .....	31
5.2.3 Hyperparameter tuning of decision tree .....	32
5.2.4 Hyperparameter tuning of random forest .....	33
5.3 Electrical parameter predictions .....	34
5.3.1 Artificial neural network .....	34
5.3.2 Other machine learning models .....	37
5.4 Loss predictions .....	40
5.4.1 Artificial neural network .....	40
5.4.2 Other machine learning models .....	42
6. Conclusions and Future Work .....	46
6.1 Summary of result .....	46
6.2 Contribution to sustainability .....	47
6.3 Ethics .....	48
6.4 Future work .....	48
References .....	50

## List of Figures

Fig.1 The basic architecture of neural network.

Fig.2 Example of k-nearest neighbors ( $k = 3$ ).

Fig.3 The architecture of decision tree model.

Fig.4 A basic random forest structure.

Fig. 5 k-fold cross validation.

Fig.6 Cross section of PMSM architecture.

Fig.7 Boxplots of the raw input data (left) and the normalized input data (right) for electrical parameters prediction.

Fig.8 Boxplot of the output data for electrical parameters prediction.

Fig.9 Scatter plot matrix of the input and output variables.

Fig.10 Correlation matrix of the normalized input data for electrical parameters prediction.

Fig.11 Explained variance ratio (left) and cumulative explained variance (right) in the normalized input for electrical parameters prediction.

Fig.12 Boxplots of the raw input data (left) and the normalized input data (right) for loss prediction.

Fig.13 Boxplot of the output data for loss prediction.

Fig.14 Scatter plot matrix of the input and output variables.

Fig.15 Correlation matrix of the normalized input data for loss prediction.

Fig.16 Explained variance ratio (left) and cumulative explained variance (right) in the normalized input for loss prediction.

Fig.17 Relationships of predicted values and actual values of electromagnetic torque ( $T_q$ ), direct-axis voltage ( $U_d$ ), and quadrature-axis voltage ( $U_q$ ) using artificial neural network with default parameters.

Fig.18 Relationships of predicted values and actual values of electromagnetic torque ( $T_q$ ), direct-axis voltage ( $U_d$ ), and quadrature-axis voltage ( $U_q$ ) using k-nearest neighbors with initial hyperparameters.

Fig.19 Relationships of predicted values and actual values of electromagnetic torque ( $T_q$ ), direct-axis voltage ( $U_d$ ), and quadrature-axis voltage ( $U_q$ ) using decision tree with initial hyperparameters.

Fig.20 Relationships of predicted values and actual values of electromagnetic torque ( $T_q$ ), direct-axis voltage ( $U_d$ ), and quadrature-axis voltage ( $U_q$ ) using random forest with initial hyperparameters.

Fig.21 Relationships of predicted values and actual values of electric machine loss ( $P_{machine}$ ), inverter loss ( $P_{inv}$ ), and power difference between electromagnetic power and mechanical power ( $P_{diff}$ ) using artificial neural network with initial hyperparameters.

Fig.22 Relationships of predicted values and actual values of electric machine loss ( $P_{machine}$ ), inverter loss ( $P_{inv}$ ), and power difference between electromagnetic power and mechanical power ( $P_{diff}$ ) using k-nearest neighbors with initial hyperparameters.

Fig.23 Relationships of predicted values and actual values of electric machine loss ( $P_{machine}$ ), inverter loss ( $P_{inv}$ ), and power difference between electromagnetic power and mechanical power ( $P_{diff}$ ) using decision tree with initial hyperparameters.

Fig.24 Relationships of predicted values and actual values of electric machine loss ( $P_{machine}$ ), inverter loss ( $P_{inv}$ ), and power difference between electromagnetic power and mechanical power ( $P_{diff}$ ) using random forest with initial hyperparameters.

Fig.25 Relationship of predicted values and actual values of electromagnetic torque ( $T_q$ ), direct-axis voltage ( $U_d$ ), and quadrature-axis voltage ( $U_q$ ).

Fig.26 Residual plot of electromagnetic torque.

Fig.27 Residual plot of direct-axis voltage.

Fig.28 Residual plot of quadrature-axis voltage.



Fig.29 Relationship between predicted values and actual values of electromagnetic torque ( $T_q$ ), direct-axis voltage ( $U_d$ ), and quadrature-axis voltage ( $U_q$ ) in random forest.

Fig.30 Relationship between predicted values and actual values of electromagnetic torque ( $T_q$ ), direct-axis voltage ( $U_d$ ), and quadrature-axis voltage ( $U_q$ ) in decision tree.

Fig.31 Relationship between predicted values and actual values of electromagnetic torque ( $T_q$ ), direct-axis voltage ( $U_d$ ), and quadrature-axis voltage ( $U_q$ ) in k-nearest neighbors.

Fig.32 Relationship between predicted values and actual values of electromagnetic torque ( $T_q$ ), direct-axis voltage ( $U_d$ ), and quadrature-axis voltage ( $U_q$ ) in multiple linear regression with a quadratic model.

Fig.33 Relationship of predicted values and actual values of electric machine loss ( $P_{machine}$ ), inverter loss ( $P_{inv}$ ), and power difference between electromagnetic power and mechanical power ( $P_{diff}$ ).

Fig.34 Residual plot of the electric machine loss.

Fig.35 Residual plot of the inverter loss.

Fig.36 Residual plot of power difference between electromagnetic power and mechanical power.

Fig.37 Relationship between predicted values and actual values of electric machine loss ( $P_{machine}$ ), inverter loss ( $P_{inv}$ ), and power difference between electromagnetic power and mechanical power ( $P_{diff}$ ) in random forest.

Fig.38 Relationship between predicted values and actual values of electric machine loss ( $P_{machine}$ ), inverter loss ( $P_{inv}$ ), and power difference between electromagnetic power and mechanical power ( $P_{diff}$ ) in decision tree.

Fig.39 Relationship between predicted values and actual values of electric machine loss ( $P_{machine}$ ), inverter loss ( $P_{inv}$ ), and power difference between electromagnetic power and mechanical power ( $P_{diff}$ ) in k-nearest neighbors.

Fig.40 Relationship between predicted values and actual values of electric machine loss ( $P_{\text{machine}}$ ), inverter loss ( $P_{\text{inv}}$ ), and power difference between electromagnetic power and mechanical power ( $P_{\text{diff}}$ ) in multiple linear regression with a quadratic model.

## List of Tables

Table.1 The default parameters of artificial neural network.

Table.2 The default parameters of k-nearest neighbors.

Table.3 The default parameters of decision tree.

Table.4 The default parameters of random forest.

Table.5 Electrical parameter prediction results of artificial neural network (ANN), random forest (RF), decision tree (DT), k-nearest neighbors (kNN) with default parameters.

Table.6 Loss prediction results of artificial neural network (ANN), random forest (RF), decision tree (DT), k-nearest neighbors (kNN) with default parameters

Table.7 grid search conditions and the results of artificial neural network.

Table.8 The electrical parameter prediction results of artificial neural network with optimized and initial hyperparameters.

Table.9 The loss prediction results of artificial neural network with optimized and initial hyperparameters.

Table.10 grid search conditions and the results of k-nearest neighbors regression.

Table.11 The electrical parameters prediction results of k-nearest neighbors with optimized and initial hyperparameters.

Table.12 The loss prediction results of k-nearest neighbors with optimized and initial hyperparameters.

Table.13 grid search conditions and the results of decision tree regression.

Table.14 The electrical parameters prediction results of decision tree with optimized and initial hyperparameters.

Table.15 The loss prediction results of decision tree with optimized and initial hyperparameters.

Table.16 grid search conditions and the results of random forest regression.

Table.17 The electrical parameters prediction results of random forest with optimized and initial hyperparameters.

Table.18 The loss prediction results of random forest with optimized and initial hyperparameters.

Table.19 Prediction results of artificial neural network model.

Table.20 Prediction results of artificial neural network (ANN), random forest (RF), decision tree (DT), k-nearest neighbors (kNN), and multiple linear regression with a quadratic model (MLR).

Table.21 Prediction results of artificial neural network.

Table.22 Prediction results of each model.

## Terminology

### A

ANN  
Artificial Neural Network.....1

AC  
Alternating Current .....1

### D

DC  
Direct Current.....1

DT  
Decision Tree.....1

### E

EV  
Electric Vehicle .....1

### K

KNN  
K-Nearest Neighbors .....1

### M

MAPE  
Mean Absolute Percentage Error .....1

MSE  
Mean Squared Error .....1

MLR  
Multiple Linear Regression.....1

### P

PMSM  
Permanent Magnet Synchronous Machine.....1

### R

RF  
Random Forest .....1

# 1. Introduction

In this chapter, The research problem and background are explained in the first part, and then the aim and objectives are described. In the end, the scope and limitations of the project are described.

## 1.1 Research problem

Permanent Magnet Synchronous Machines (PMSMs), which include high efficiency, high power density, wide speed range, and fast dynamics, have led to a growing interest in them (An et al. 2021). They have demonstrated the most superior overall performance for Electric Vehicles (EVs) in recent times (Ni et al. 2014). However, PMSMs exhibit significantly non-linear magnetic features because of the presence of reluctance torque and the presence of nonlinearity makes it challenging to create models.

In this research project, to predict the parameters and losses in the nonlinear systems, artificial neural network and machine learning models are developed as new prediction approaches for the Volvo Cars' PMSM and their performances are evaluated while comparing them.

Volvo Cars has a goal to transform the conventional car manufacturing industry into a sustainable, interconnected, and intelligent future. With a long history of prioritizing safety and inventing user-friendly cars, Volvo Cars made a decision in 2010 to completely overhaul their business, introducing a fresh fleet of cars and technology, leading to ongoing progress and outstanding sales. Their aim is to sell 1.2 million cars annually by 2025, with 50% being electric vehicles and sold online to customers. Volvo Cars' Electric Drive team is in charge of creating and providing effective solutions for the inverters, electric machines, and transmission of electric vehicles. Volvo Cars aims to be at the forefront of electrification, prioritizing energy efficiency, sustainability, customer satisfaction, and optimal performance and drivability in all of their upcoming products. Their ultimate goal is to establish themselves as a leader in the field of electrification.

In order to accomplish the goal, it is one of the vital factors to evaluate an E-machine's electrical characteristics and losses accurately and predict system performance and secure a safe and reliable system operation.

## 1.2 Aim and objectives

The main aim of this project is to predict electrical parameters and losses of EVs precisely to anticipate its performance and secure that the system operates safely and reliably. The electrical parameters includes electromagnetic torque, direct-axis voltage, and quadrature-axis voltage. The losses includes electric machine loss, inverter loss, and power difference between electromagnetic power and mechanical power. The objectives are:

- Objective1: Preprocess dataset to train and evaluate neural network models
- Objective2: Develop neural network and machine learning models to predict electrical parameters and losses of EVs
- Objective3: Improve the accuracy of the models to anticipate parameters and losses accurately
- Objective4: Evaluate the performances of each model

## 1.3 Scope and limitations

The primary scope of the project is to predict electrical parameters and losses accurately by developing neural network models. The test data that can be used for training and evaluation is limited to PMSMs made of Volvo cars. The test data conditions are also restricted. The data that is used for parameter prediction is at 30, 60, and 90 degree Celsius, and the shaft rotation speed is 1000 rpm, direct current (DC) voltage is 370 Vdc. The data that is utilized to predict losses is at 30 and 60 degree Celsius with three different DC voltage such as 350 Vdc, 400 Vdc, and 450Vdc and the shaft rotation speed is 1000 rpm to 14000 rpm. Although the electrical parameter prediction model is trained only on data with a shaft rotation speed of 1000 rpm, the dataset for loss prediction includes data from 1000 rpm to 14000 rpm, so the predicted value of electromagnetic torque used to calculate the power difference in the loss prediction model might not be appropriate, especially when the shaft speed is much higher than 1000 rpm.

The amount of the available test data is also one of the limitations. Hyperparameters of each model that can be adjusted in this project are also limited. There are a number of machine learning algorithm but the models selected in this project are artificial neural network, k-nearest neighbors, decision tree, random forest, and multiple linear regression with a quadratic model.

## 2. Theoretical Framework

Theoretical frameworks that are used in the project are described in this chapter. Neural network algorithm including feedforward and backpropagation process is explained in the first part. Other machine learning algorithms such as k-nearest neighbors, decision tree regression, and random forest regression and multiple linear regression with a quadratic model are described in the following part. In addition, cross validation and hyper parameter tuning techniques are described in the end part.

### 2.1 Artificial neural networks

Artificial neural network have applied for a wide range of uses such as image recognition, pattern recognition, natural language processing, defect detection, and forecasting (Montavon et al. 2018). Due to its capacity to automatically acquire features and carry out high-volume modeling, neural networks are an advanced analytics tool that is beneficial in the age of big data (Wu et al. 2017). The MP model and the Hebb rule were put forth in the 1940s to explore how neurons function in the human brain (Clark et al. 2013). Additionally, a chess playing and elementary logic problem-solving artificial intelligence was created (Samuel 1988).

Artificial neural networks are composed of adaptable units known as artificial neurons, which possess modifiable parameters. These neurons are capable of performing simultaneous computations for the purpose of data processing (Kocak and Siray 2021). Neurons in a neural network are divided into layers, and each layer performs a specific type of computation. The first layer receives input data, which is called input layer. One or more hidden layers use the output of the input layer to run different calculations on the input data. The final result of the network is produced at the last layer that is called the output layer. In a neural network, the connections between the neurons are weighted, which means that the intensity of each connection is determined by a numerical value. To minimize the discrepancy between the network's output and the desired output for a particular input, the weights of the connections are modified during training. Neural network has two main process in each iteration including feedforward and back propagation.



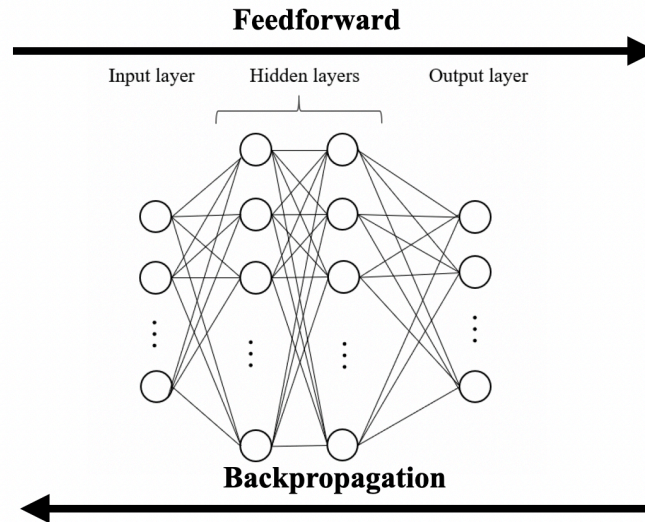


Fig.1 The basic architecture of neural network

### 2.1.1 Feedforward process

Each edge between each neuron have specific weight. The output of each neuron in a layer is computed by taking a weighted sum of its inputs, applying an activation function to the result, and passing the output to the next layer. The activation function adds nonlinearity and aids in capturing intricate connections between the input and output variables. The computing process can be represented as the following equations:

$$z = Wx + b$$

where  $W$  represents the weight matrix,  $x$  denotes the input, and  $b$  represents the bias.

$$a = f(z)$$

where  $f$  is the activation function and  $a$  is the output of the neuron. The activation function of hidden layers are ReLU function and that of output layer is linear function in the neural network model of this project. ReLU function can be represented as the following equation:

$$f(x) = \max(0, x)$$

The output is utilized for the computation in the next layer as the input. This process is repeated until output is obtained from the output layer.

### 2.1.2 Backpropagation

Backpropagation algorithm was created in 1974 to address a nonlinear neural network issue (Werbos 1990). By adjusting the weights and biases of the neurons, the error is minimized. The error is the difference between true output and neural network's predicted output, which is also called loss function. Mean squared error (MSE) is used in the artificial neural network model developed in the project. The weights and biases are updated from the output layer to the input layer. The weights and biases of each neuron in the network are updated based on the error calculated during backpropagation. The update process of the weights and biases can be represented as the following:

$$w_{new} = w_{old} - \eta \frac{\partial E}{\partial w}$$

$$b_{new} = b_{old} - \eta \frac{\partial E}{\partial b}$$

where  $w_{new}$  is updated weight,  $w_{old}$  denotes weight before update,  $\eta$  is learning rate  $b_{new}$  represents updated bias, and  $b_{old}$  denotes bias before update. The amount of adjustment to the weights and biases is determined by a learning rate, which controls how much the weights and biases are changed during each iteration of the backpropagation algorithm. The process of feedforward calculation, loss function calculation, and backpropagation is repeated for a certain number of epochs.

## 2.2 K-nearest neighbors regression

K-nearest neighbors is one of the simplest and oldest classification algorithms which works for both regression and classification (Gou et al. 2012). It is calculated using Euclidean distance from a simple majority vote of the  $k$  closest neighbors of each point. Because it does not train the model instead just stores instances of the training data, it is also known as lazy learning. The example of k-nearest neighbors is illustrated in Fig.2. In this example the number of neighbors  $k$  is 3, therefore, the average value of three nearest points from feature  $x_1$  becomes the predicted value for  $x_1$ .

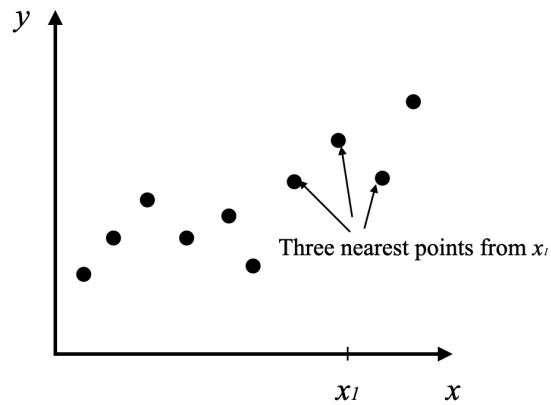


Fig.2 Example of k-nearest neighbors ( $k = 3$ ).

### 2.3 Decision tree regression

The decision tree generates a set of criteria for classification that can be applied to the data (Bel 2009). In order to minimize a heterogeneity criterion that is derived on the resulting sub-leaves, it constructs a binary tree by recursive binary partitioning that splits a subset of the dataset into two subsets. The architecture of decision tree is illustrated in Fig.3. For the criterion, mean squared error is used in this report. The method is easy to grasp and visualize but it can result in intricate trees that are challenging to generalize. Additionally, it might be unstable because even minor changes in the dataset could result in completely different trees.

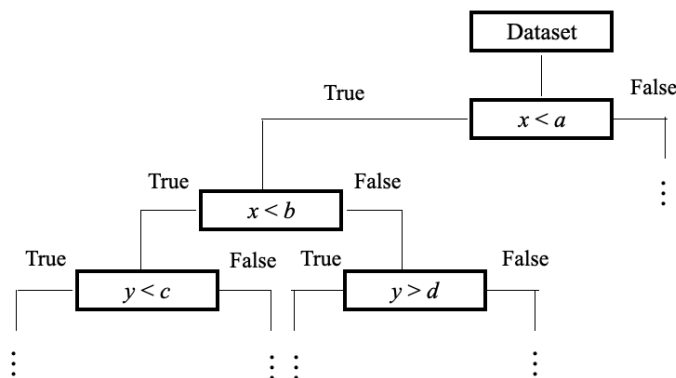


Fig.3 The architecture of decision tree model.

## 2.4 Random forest regression

The random forest algorithm is a classification and regression method proposed in 2001 (Breiman 2001). Fig.4 Shows a basic structure of random forest. The random forest usually contains hundreds or thousands of decision trees on various different sub-samples of datasets. In order to improve the model's accuracy, it utilizes averages of each decision tree results (Badillo et al. 2021). By averaging the outputs of various decision trees, it can control overfitting.

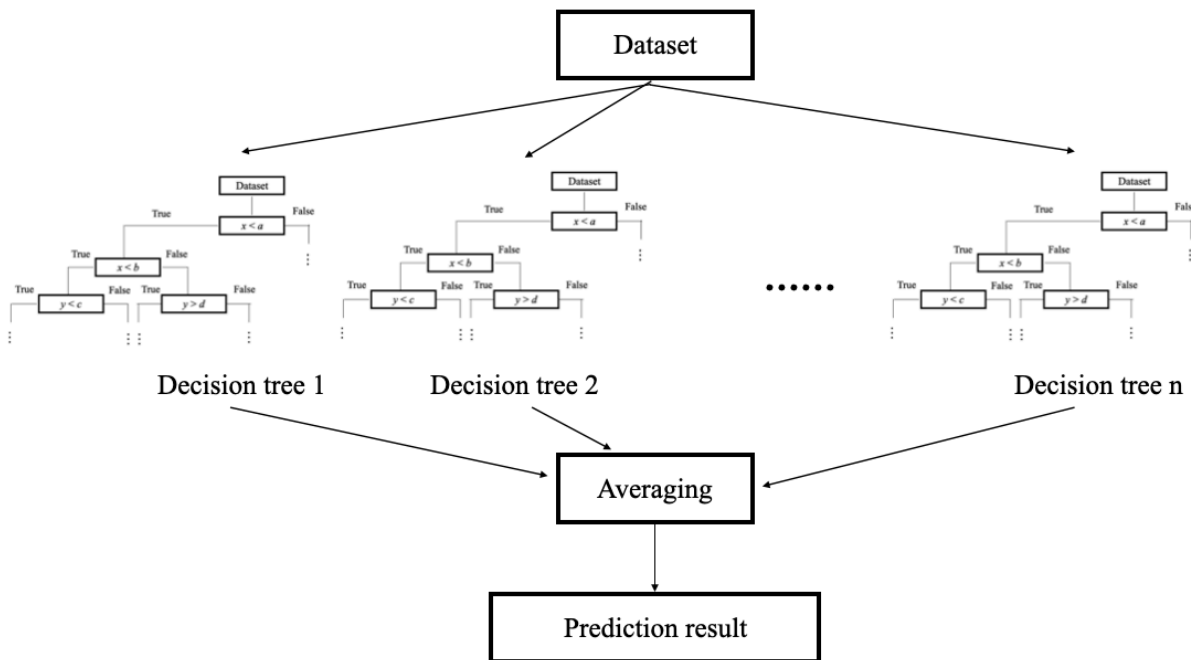


Fig.4 A basic random forest structure.

## 2.5 Multiple linear regression with a quadratic model

Quadratic model expands the notion of linear regression and enables the modeling of nonlinear interactions between the variables by adding quadratic factors. A general form of multiple linear regression with a quadratic model with  $n$  features can be represented as the following equation:

$$y = \beta_0 + \beta_1 x_1 + \beta_2 x_2 + \dots + \beta_n x_n + \beta_{11} x_1^2 + \beta_{22} x_2^2 + \dots + \beta_{nn} x_n^2 + \epsilon$$

Where  $y$  represents dependent variable,  $x_1, x_2, \dots, x_n$  denote independent variables,  $\beta_0, \beta_1, \beta_2, \dots, \beta_n$  represent the regression coefficients,  $\beta_{11}, \beta_{22}, \dots, \beta_{nn}$  denote the coefficients for the quadratic terms, and  $\epsilon$  is the error term.

## 2.6 Cross validation

There are several types of validation techniques to evaluate the machine learning model performance and generalization ability of predictive models. In hold-out validation, the dataset is divided into two parts and one part is used for training and the other part used for validation (Shalev-Shwartz and Ben-David 2014). Fig.5 illustrates k-fold cross validation. In k-fold cross validation, the dataset is divided into  $k$  subset. The union of  $k-1$  subset is utilized for training and the remaining subset is used for testing to assess the model. The process is repeated  $k$  times while using different dataset for testing. In one-fold validation, the entire dataset is used for training without a validation set. In this report, 5-fold cross validation was implemented.

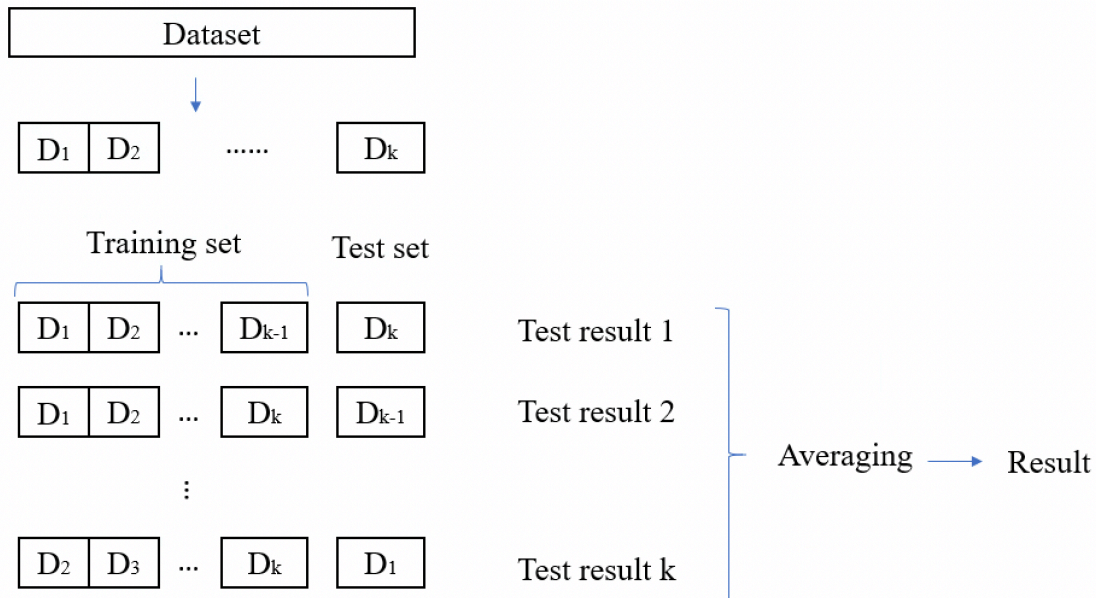


Fig. 5 k-fold cross validation.

## 2.7 Hyperparameter tuning

There are various hyperparameter optimization methods such as grid search, random search, and genetic algorithm. The hyperparameter tuning is essential to optimize the performances of the predictive models. Grid search is one of the traditional hyperparameter tuning methods. It merely conduct a full search over a predetermined portion of the training algorithm's hyperparameters domain (Liashchynskiy and Liashchynskiy 2019). In random search method, hyperparameters are chosen at random from a predetermined search area. The genetic algorithm contains four operations

including selection, crossover, mutation, and replacement, which is inspired by genetic evolution. In the process, individuals are chosen from the population based on their fitness value, and then crossover and mutation processes are used to create new individuals. After that, the new individuals replaces the parent individuals based on the replacement strategies. This process is repeated over a number of generations until the stopping criterion are achieved. In this project grid search method with 5-fold cross validation is executed to optimize hyperparameters of each regression model.

### **3. Literature Review and Related Works**

In this chapter, reviews on literature and related work are conducted. In the first section, literature on machine learning and artificial neural network are explained. Literatures about industrial applications of machine learning and deep learning are described in the next section. In the final part, the literature reviews on the PMSM prediction research using artificial neural network and machine learning are described.

#### **3.1 Machine Learning**

Supervised learning, unsupervised learning, semi-supervised learning, and reinforcement learning are the four primary categories of machine learning algorithms (Shalev-Shwartz and Ben-David 2014).

Supervised learning involves using example input-output pairs to learn a function that maps an input to an output (Han et.al 2012). Supervised learning utilizes labeled data so it is conducted when a certain goal to be achieved from a certain set of inputs is identified (Sarker et.al 2020). The main purposes of supervised learning are regression and classification. Unsupervised learning uses unlabeled data. It is mainly used for clustering, dimensionality reduction, and finding association rules. Semi-supervised learning is a hybrid technique supervised learning and unsupervised learning so it learns from both labeled and unlabeled data (Sarker et.al 2020). Reinforcement learning enables software agents and computers to automatically assess the optimal behavior in a given context or environment to increase its efficacy (Kaelbling et.al 1996). The main goal of this reward or penalty learning approach is to use the knowledge gained from environmental action to take steps that either increase rewards or reduce risks (Mohammed et.al 2016). Deep learning is a part of artificial neural network techniques and it outperforms typical machine learning techniques in a variety of situations, especially when learning from huge datasets (Xin et.al 2018).

#### **3.2 Artificial neural network and machine learning for industrial applications**

Various types of applications of deep learning and machine learning are developed in the modern world.

One of the main machine learning application area is data-driven predictive analytics for intelligent decision making (Mahdavinejad et.al 2018). Several machine learning and artificial neural network algorithms are used for the purpose.

Nguyen et al. (2020) predicted tensile and compressive strengths of high-performance concrete using four different machine leaning methods such as multilayer perceptron, support vector regression, extreme gradient boost, and gradient boosting regressor. The gradient boosting regressor and extreme gradient boost models are shown better performance than the other models. Cappugi et al. (2021) developed a model that can predict energy yield losses of wind turbine based on the severity of leading edge erosion damage by combining artificial neural networks, Navier–Stokes computational fluid dynamics, and blade element momentum theory of wind turbine engineering.

Because precise predictions offer knowledge about the future, they can help almost any industry, company, or organization make better decisions. This includes government agencies, online shopping, banking and financial services, medical care, advertising and marketing, transportation, and a wide range of other industries (Sarker 2021).

Image recognition that recognize something as a digital image is also common usage of machine leaning (Fujiyoshi et al. 2019). Traditional techniques of image recognition are a combination of feature extraction method such as histogram of gradient and machine learning algorithm like support vector machine. Image recognition approaches based on deep learning are convolutional neural networks that is used for several applications such as image classification, object detection, and semantic segmentation. To determine whether an x-ray is carcinogenic or not, object detection, face detection, and tag recommendations in an image are the examples. Another widely used technology of machine learning is speech recognition, which usually utilizes linguistic and acoustic models (Chiu et.al 2018). For example, Alexa, Siri, and Cortana utilizes these machine learning methods. Chiu et.al developed a neural network model that combines the acoustic, pronunciation, and language models for sequence-to-sequence speech recognition by improving Listen, Attend, and Spell model in their research. In addition, pattern recognition is one of the popular applications of machine learning, which identify the regularities and trends in data automatically (Bishop et.al 2006). There are various pattern recognition models such as kernel methods, neural networks, Hidden Markov Models.



### **3.3 Artificial neural network and other machine learning for PMSM parameters and losses prediction**

Machine learning and Neural network are also applied to predict PMSM parameters and losses.

Yan et al. (2019) developed a neural network for predicting electromagnetic torque of PMSMs. The inputs have four variables including direct and quadrature axis current, the rotor position, and rotor's angular velocity. The neural network model achieved 98.3% accuracy by optimizing learning rate, batch size of training, and the number of hidden layers. The neural network has simple architecture and good accuracy and it can train for a short time.

He et al. (2022) proposed a neural network model including BP neural network and deep belief network to predict losses and electromagnetic torque of PMSMs. The neural network has two hidden layers and four inputs such as rib, magnets width, magnets thickness, and air gap length. The accuracy of 95% was reached for predicting electromagnetic torque. The prediction results of the rotor core loss and stator core loss showed 14% and 20 % errors respectively.

Bingi et al (2021) developed a neural network model to predict torque and temperatures of PMSMs. The temperatures includes stator yoke, stator tooth, magnet surface, and stator winding. The inputs of the model are ambient temperature coolant temperature, direct-component of voltage, quadrature-component of voltage motor speed, direct-component of current, and quadrature component of current. By tuning the number of hidden layers, the number of neurons, the number of epochs, and training algorithm, the mean squared error of 0.0003 and 0.0001 are achieved. The activation function for the hidden layers of the neural network are sigmoid functions, that for the output layer is linear function.

Nawae and Thongpull (2020) built linear regression, stepwise regression, and artificial neural network regression models for torque prediction. The park transformation of current, the clarke transformations of voltage and current, and shaft speed are used as inputs. Among the three models, the result shows that the neural network model reached the highest accuracy with the R-squared score of 0.996.

Guo et al. (2020) developed artificial neural network, support vector machine, random forest and adaboost ensemble learning, decision tree, and ridge regression to predict winding temperature of

stator. Input of the model includes direct axis current and voltage, quadrature axis current and voltage, motor torque, motor temperature, motor speed, ambient temperature, stator yoke temperature, and stator tooth temperature. The artificial neural network model indicates the best performance in comparison with other machine learning methods. The accuracy of the neural network model shows around 85%.

Taking advantage of the prediction possibility of the artificial neural network and machine learning techniques, these methods are developed for the electric machine of Volvo Cars Corporation as a new approach to predict its electric parameters and losses in this project.

## 4. Experimental Methodology

In this chapter, the experimental methodology implemented in the research are described, which includes data collection, develop prediction models such as machine learning and artificial neural network, and evaluation methods of the models.

Python is the programming language used for the experiments. The ‘sklearn’ library is used for splitting the dataset and developing machine learning models including k-nearest neighbors, decision tree, random forest, and multiple linear regression with a quadratic model. Additionally, the ‘sklearn’ library is utilized for the model evaluation with mean squared error, mean absolute error, and coefficient of determination. Moreover, the ‘tensorflow’ and ‘keras’ libraries are used for developing artificial neural network models and the ‘seaborn’ library is utilized to produce the correlation maps and scatter plot matrices. The computer specifications is that the OS is macOS Venture 13.4, the CPU is Apple M1 chip, and the memory is 16 GB.

### 4.1 Data collection and preparation

The first step is to collect test operation data from Volvo Cars Corporation’s test database. The test was implemented by Volvo Cars Corporation. By using test operation data from Volvo Cars database, input and output data for the models was computed. The test was performed for a specific PMSM (Permanent Magnet Synchronous Machine) machine. The inputs data is normalized by the following equation:

$$x_{norm} = (x - \mu) / \sigma$$

where  $\mu$  is the mean of  $x$ ,  $\sigma$  is the standard deviation of  $x$ .

The dataset is divided into subset of 60% for training, 20% for validation to evaluate model while training, and 20% for tasting to assess the model after training.

#### 4.1.1 Data for electrical parameter prediction

The cross section of PMSM, he positions of the rotor, stator winding, and permanent magnet in PMSM are illustrated in Fig.6.

The test was implemented at 1000 rpm with 370 Vdc (direct current (DC) voltage) at three different temperatures including 30, 60, and 90 degree Celsius. The dataset for electric parameter prediction includes input variables such as direct-axis (d-axis) current, quadrature-axis (q-axis) current, winding resistance, and rotor temperature, and output parameters such as direct-axis voltage, quadrature-axis voltage, electromagnetic torque. The data at 30 degree Celsius contains 2839 data points, the data at 60 degree Celsius contains 2840 data points, and the data at 90 degree Celsius includes 2201 data points. All the temperature data is used to train the model. All the temperature data including 7880 data points was used for train and evaluate the prediction models.

The boxplots is used to visualize input and output data. Fig.7 shows the boxplots of the raw input data and the normalized input data. The  $i_d$  represents d-axis current, the  $i_q$  represents q-axis current, the  $T_{rot}$  denotes the rotor temperature, the  $R_s$  denotes winding resistance. By normalizing the data, the impacts of each variable become more smooth. The boxplot of the output data is shown in Fig.8. the  $u_d$  represents d-axis voltage, the  $u_q$  denotes q-axis voltage, and the  $T_q$  is the electromagnetic torque. The value ranges of d-axis voltage and q-axis voltage are similar but electromagnetic torque has wider value range. The scatter plot matrix of the input and output variables are also described in Fig.9.

The correlation matrix of the normalized input data is illustrated in Fig.10. The matrix indicates that the low correlation pairs are d-axis current and q-axis current, d-axis current and the rotor temperature, d-axis current and the winding resistance, q-axis current and the rotor temperature, q-axis current and the winding resistance. It also shows that the rotor temperature and the winding resistance have a high correlation. It could be considered that is because the winding resistance is related to the winding temperature and the temperature is similar to the rotor temperature because they are made of metal so they have high thermal conductivity.

Principle component analysis in the normalized input is also implemented. The explained variance ratio and cumulative explained variance are shown in Fig.11. The PC1 represents d-axis current, the PC2 denotes q-axis current, PC3 represents the rotor temperature, and the PC4 is the winding resistance. The cumulative explained variance of PC1, PC2, and PC3 indicates around 98.5% so if PC4 is removed to train the model, the training time for the machine learning and deep learning models could be reduced without significant difference in the prediction results.

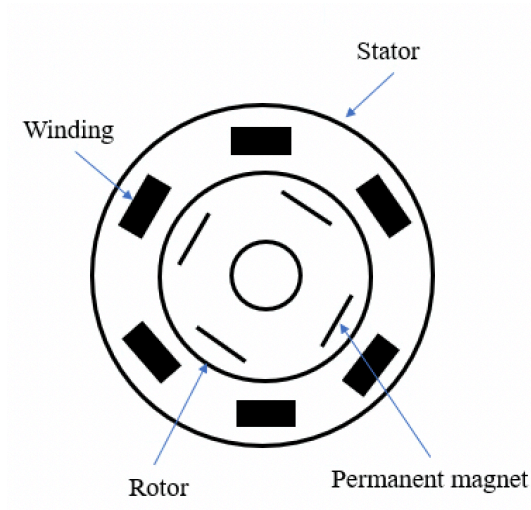


Fig.6 Cross section of PMSM architecture.

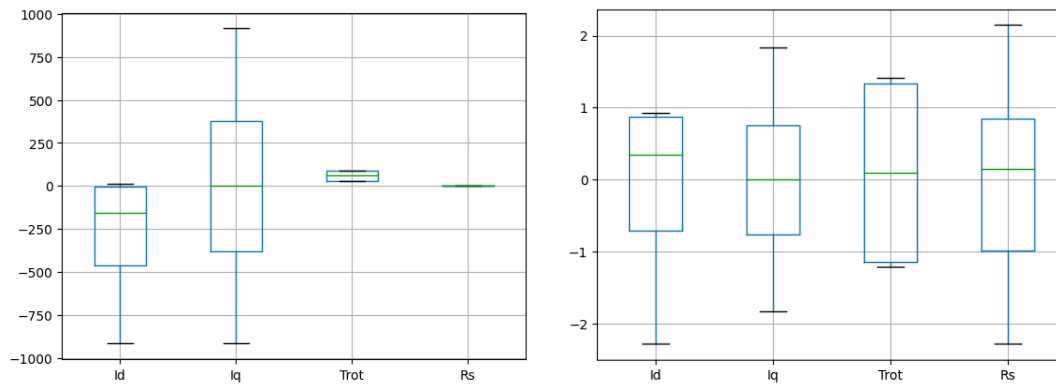


Fig.7 Boxplots of the raw input data (left) and the normalized input data (right) for electrical parameters prediction.

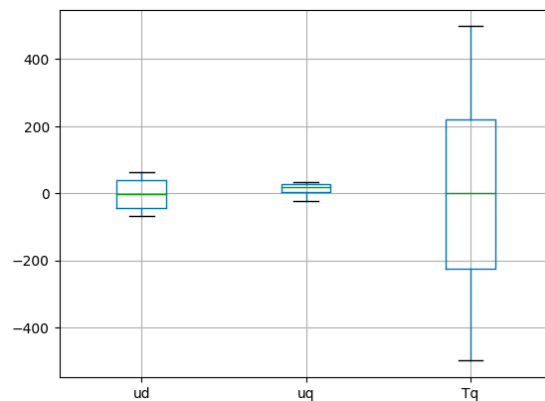


Fig.8 Boxplot of the output data for electrical parameters prediction.

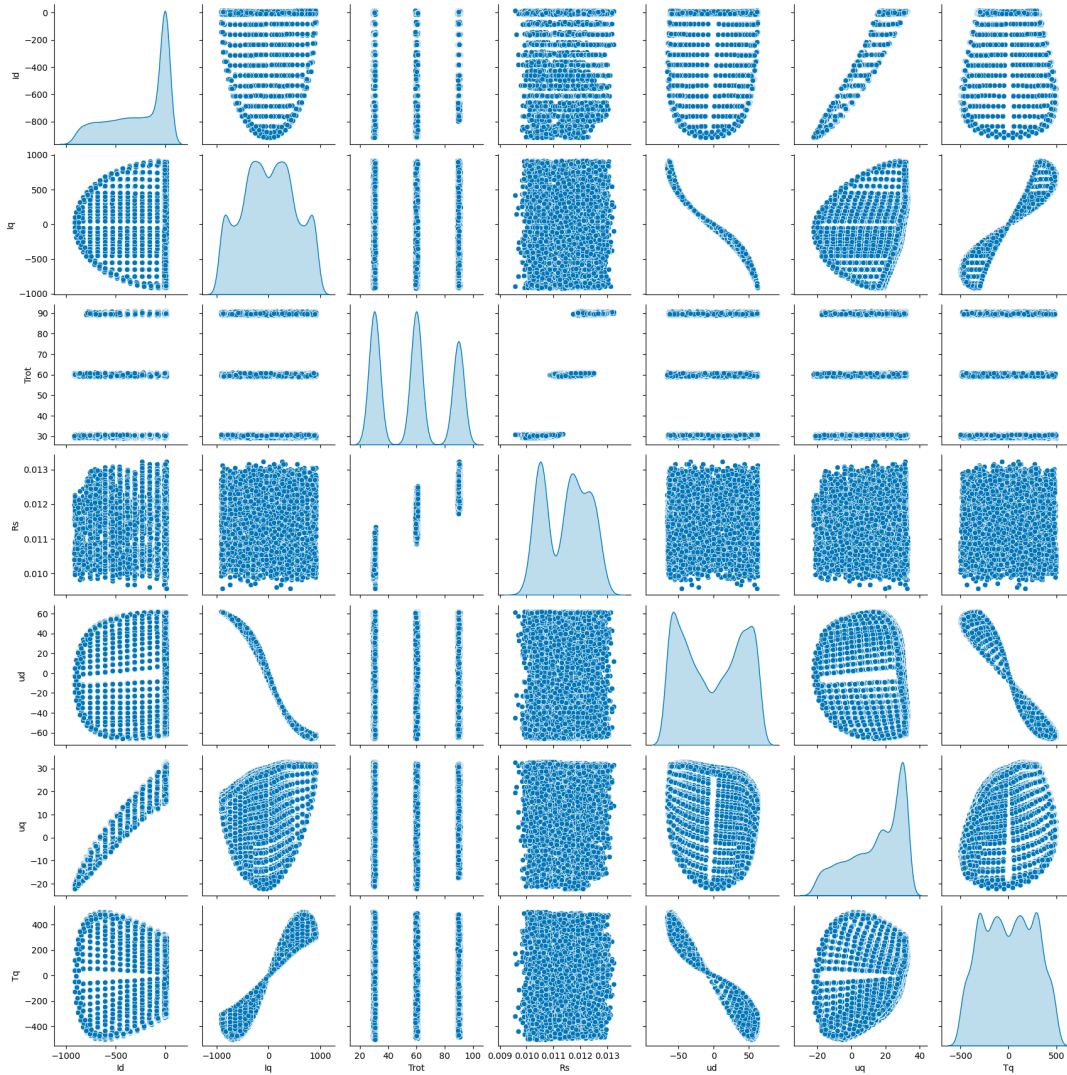


Fig.9 Scatter plot matrix of the input and output variables.

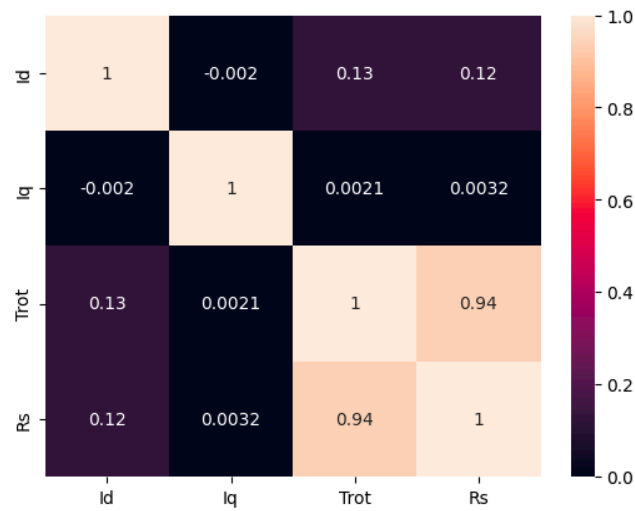


Fig.10 Correlation matrix of the normalized input data for electrical parameters prediction.

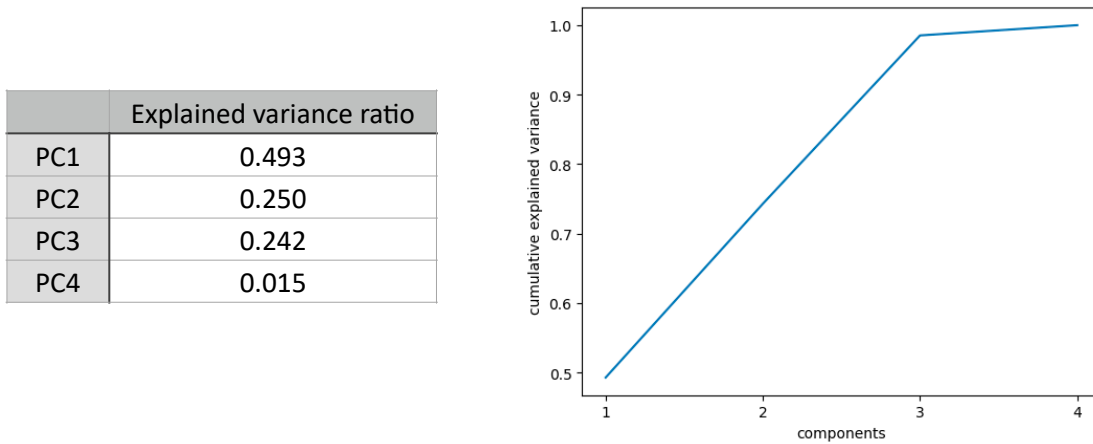


Fig.11 Explained variance ratio (left) and cumulative explained variance (right) in the normalized input for electrical parameters prediction.

#### 4.1.2 Data for loss prediction

The test was performed at three different DC (direct current) voltage including 350 Vdc, 400 Vdc, and 450Vdc with two different magnet temperature that are 30 and 60 degree Celsius at 1000 to 14000 rpm. The data at 30 degree Celsius contains 2630 data points and the data at 60 degree Celsius contains 2520 data points. The data at a both temperature including 5150 data points was used for the model training and evaluation. The data that the shaft rotation speed is 0, which means that the shaft does not move, are deleted from the data frame.

The dataset for loss prediction includes input variables such as d-axis current, q-axis current, DC voltage, winding temperature, rotor temperature, and shaft rotation speed. Also, parameters that used for output such as total electric machine loss, inverter loss, and mechanical torque are contained in the dataset. Mechanical torque and shaft rotation speed are used for calculating power difference between electromagnetic power and mechanical power that is one of the output variables. An inverter is a devise that converts direct current (DC) to alternating current (AC). Therefore, the inverter loss means the power loss during the conversion process from DC to AC. DC is converted to AC for use in electric machine. The inverter loss can represent as the following equation:

$$P_{inv} = P_{dc} - P_{ac}$$

where  $P_{inv}$  is inverter loss,  $P_{dc}$  is DC power that is input to the inverter, and  $P_{ac}$  is AC power that is output from the inverter.

The electric machine loss is the power loss in electric machine to convert AC power to mechanical output. The electric machine loss can be represent as the following equation.

$$P_{machine} = P_{ac} - P_{mech}$$

where  $P_{machine}$  is total electric machine loss and  $P_{mech}$  is mechanical power that is output from electric machine.

The power difference between electromagnetic power and mechanical power is computed by following equations:

$$T_{diff} = T_{el} - T_{mech}$$

$$P_{diff} = T_{diff} * N * \pi/30$$

where  $T_{el}$  denotes electromagnetic torque,  $N$  demotes shaft rotational speed,  $T_{diff}$  is torque difference,  $P_{diff}$  represents power difference, and  $T_{mech}$  is mechanical torque.

Fig.12 shows the boxplots of the raw input data and the normalized input data. The  $I_d$  represents d-axis current, the  $I_q$  represents q-axis current, the  $U_{dc}$  is the DC voltage, the Speed is the shaft rotation speed, the  $T_{rot}$  is the rotor temperature, the  $T_{win}$  is winding temperature. By normalizing the data, the impacts of each variable become more smooth. The boxplot of the output data is shown in Fig.13. the  $P_{inv}$  represents the inverter loss, the  $P_{machine\_2}$  denotes electric machine loss and the  $P_{diff}$  represents power difference between the electromagnetic power and the mechanical power. The value ranges of the power difference is the widest which is followed by that of the electric machine loss. Inverter losses have the narrowest value range. The scatter plot matrix of the input and output variables are also described in Fig.14.

The correlation matrix of the normalized input data is illustrated in Fig.15. The matrix shows that the rotor temperature and the winding temperature have a high correlation because the temperatures are similar due to their high thermal conductivity. The matrix also shows low correlations except for those temperatures.



Principle component analysis in the normalized input is also conducted. Fig.16 depicts the explained variance ratio and the cumulative explained variance. The PC1 represents d-axis current, the PC2 denotes q-axis current, PC3 represents the DC voltage, and the PC4 is the shaft rotation speed, the rotor temperature, and the PC4 is the winding temperature. The cumulative explained variance of PC1, PC2, PC3, PC4, and PC5 shows around 98.4%. The results indicates the training time for the machine learning and deep learning models could be reduced without significant difference in the prediction results if PC6 is removed to train the model.

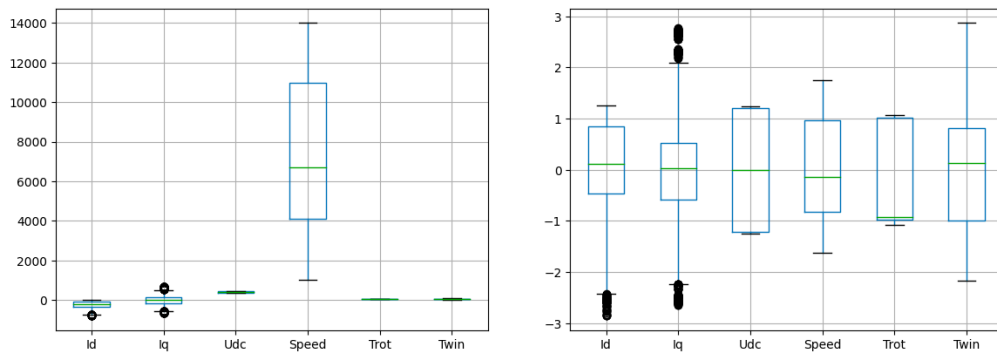


Fig.12 Boxplots of the raw input data (left) and the normalized input data (right) for loss prediction.

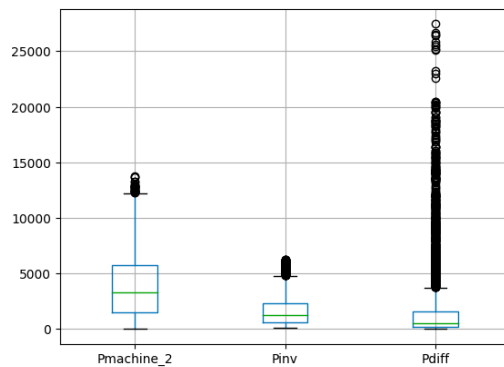


Fig.13 Boxplot of the output data for loss prediction.

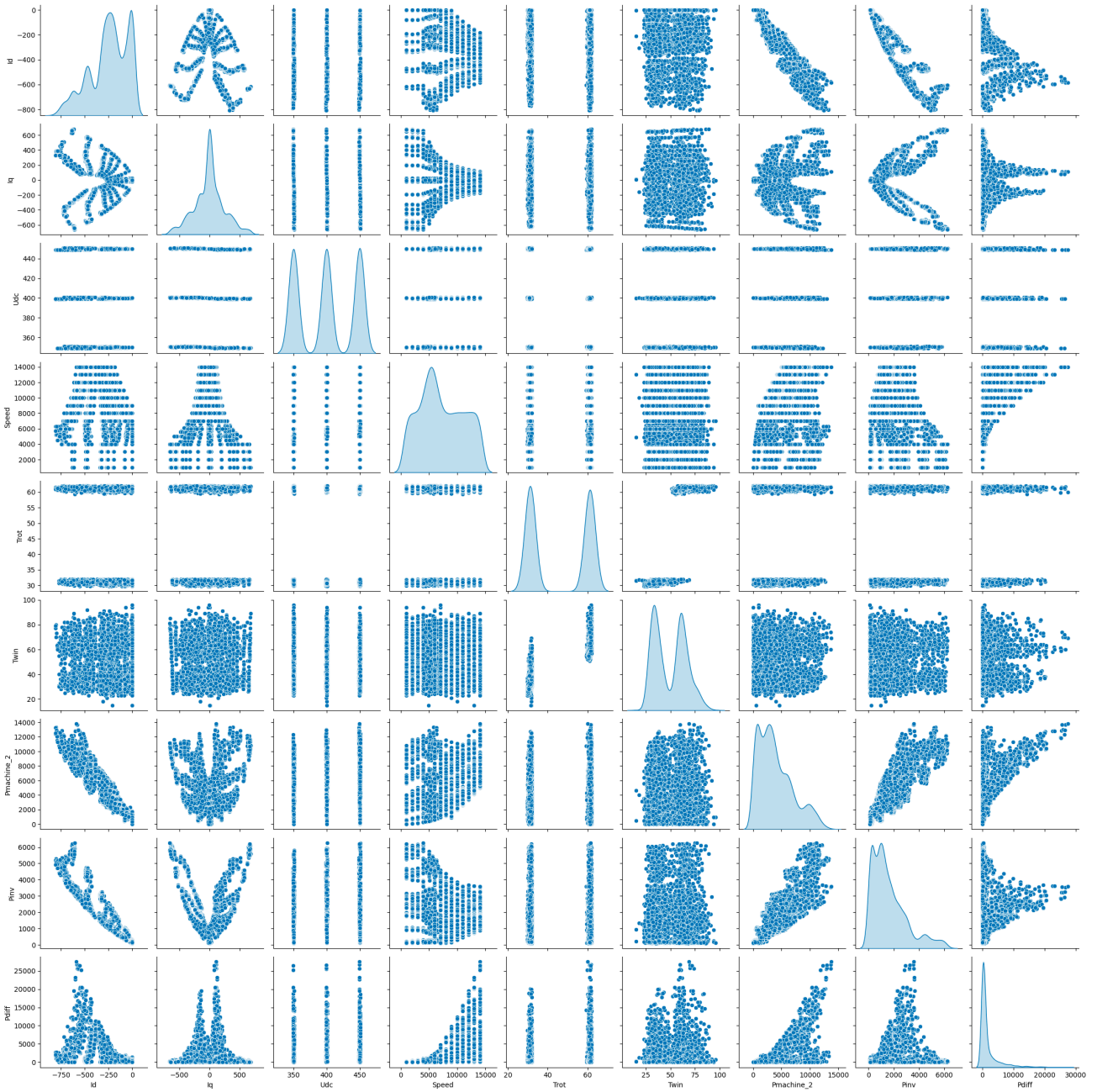


Fig.14 Scatter plot matrix of the input and output variables.

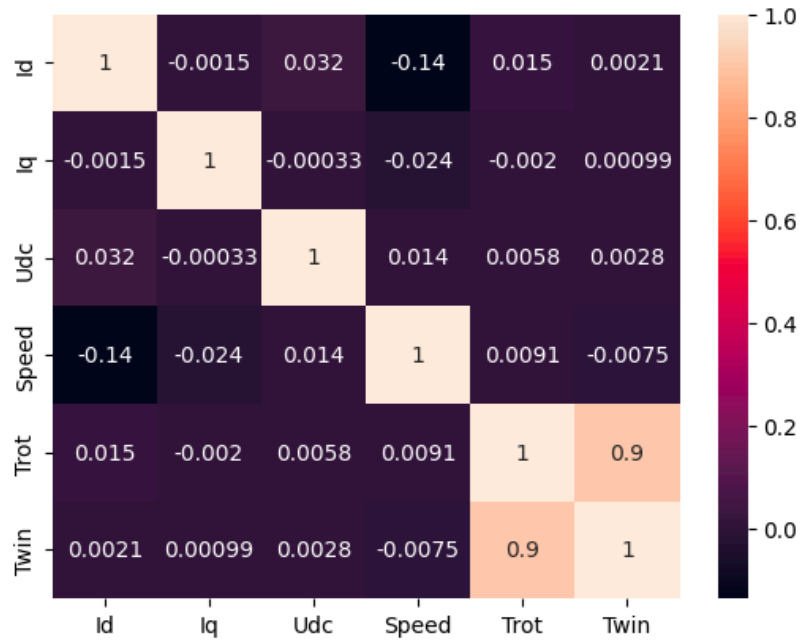


Fig.15 Correlation matrix of the normalized input data for loss prediction.

	Explained variance ratio
PC1	0.318
PC2	0.190
PC3	0.168
PC4	0.166
PC5	0.142
PC6	0.016

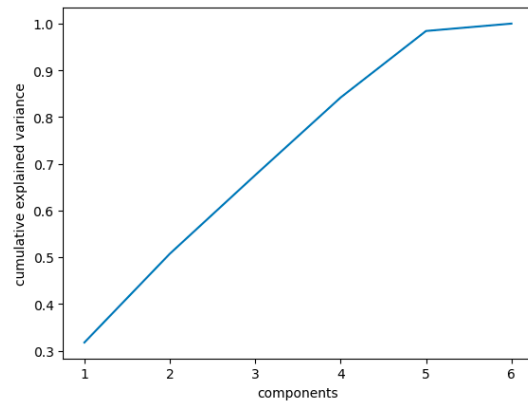


Fig.16 Explained variance ratio (left) and cumulative explained variance (right) in the normalized input for loss prediction.

## 4.2 Develop artificial neural network and machine learning models

Artificial Neural network and machine learning models are developed for predicting electrical parameters including electromagnetic torque, direct-axis voltage quadrature-axis voltage. In addition, the models to predict electrical losses including the electric machine loss and inverter loss are built.

Pre-processed data is used to train, validate, and test the artificial neural network and machine learning models. The models are optimized by hyperparameter tuning using grid search with 5-fold cross validation to minimize the prediction error of each parameter.

### **4.2.1 Hyperparameter tuning of artificial neural network**

The tuned hyperparameters using grid search with cross validation in neural network models are the following:

- The number of neurons in each hidden layer
- The number of hidden layers
- Epochs (the number of epochs): Each iteration of the given feature and target data constitutes an epoch
- Learning rate: Learning rate controls how much the weights update during each backpropagation phase
- Batch size: Batch size is the number of samples used in each compute batch

### **4.2.2 Hyperparameter tuning of k-nearest neighbors**

For k-nearest neighbors regression model, the following hyperparameters are adjusted by grid search with cross validation:

- The number of neighbors
- Weight function: the weight function is uniform or distance. When uniform is selected, each neighborhood's points are given equal weight. When distance is chosen, a query point's closer neighbors will be of greater impact than its farther neighbors.
- Power parameter: the power parameter is manhattan distance or euclidean distance. When  $p=1$ , Manhattan distance is used and when  $p=2$ , euclidean distance is used.

### **4.2.3 Hyperparameter tuning of decision tree**

The following hyperparameters in decision tree regression model are optimized using grid search with cross validation:

- The maximum depth of the tree (max\_depth)

- The minimum number of samples needed to divide internal node (min\_samples\_split)
- The minimum number of samples required to be at a leaf node (min\_samples\_leaf)
- The number of features to take into account while choosing the best split (max\_features): [when 'sqrt' is selected, sqrt(n\_features) is used, when 'log2' is chosen, log2(n\_features) is used, if None is selected, n\_features is utilized.

#### 4.2.4 Hyperparameter tuning of random forest

The following hyperparameters in random forest regression model are tuned using grid search with cross validation:

- The number of decision trees in the random forest (n\_estimators):
- The maximum depth of the decision trees (max\_depth)
- The minimum number of samples required to split an internal node (min\_samples\_split)

### 4.3 Model evaluation

The performance of the trained neural network model are evaluated based on its accuracy in predicting the PMSM's electrical parameters and losses under a variety of test operation conditions. Mean squared error (MSE), coefficient of determination ( $R^2$ ) and mean absolute percentage error (MAPE) are utilized for measuring the performances. MSE, MAPE and  $R^2$  can be represented as the following:

$$MSE = \frac{1}{n} \sum_{i=1}^n (y_i - \hat{y}_i)^2$$

$$MAPE = \frac{1}{n} \sum_{i=1}^n \left| \frac{y_i - \hat{y}_i}{y_i} \right| \times 100 \%$$

$$R^2 = 1 - \frac{\sum_{i=1}^n (y_i - \hat{y}_i)^2}{\sum_{i=1}^n (y_i - \bar{y})^2}$$

where  $\hat{y}_i$  is predicted output value,  $\bar{y}$  is average value of training data.

Additionally, the relationship between predicted values and actual values of each target variables such as electromagnetic torque, d-axis voltage, and q-axis voltage are shown to make results

understandable visually. Moreover, in order to support the results visually, residual plots of each target variables, including electric machine loss and the inverter loss, are also depicted. The results of each model are compared to assess which algorithms performed better for each prediction.

## 5. Results and Discussion

The results of the prediction models with default parameter at the beginning in this chapter. The results of hyperparameter tuning and prediction results of electrical parameters and loss are described in the subsequent part.

### 5.1 Prediction results with default parameter

The default parameters of artificial neural network, k-nearest neighbors, decision tree, and random forest models are shown in Table.1, Table.2, Table.3, and Table.4, respectively. The electrical parameter prediction results of artificial neural network and other machine learning models with default parameters are illustrated in Table.5.

The relationships of predicted values and true values of the electrical parameters including electromagnetic torque, direct-axis voltage, and quadrature-axis voltage using artificial neural network, k-nearest neighbors, decision tree, and random forest models with the default parameters are depicted in Fig.17, Fig.18, Fig.19, Fig.20, respectively.

The loss prediction results of artificial neural network and other machine learning models with default parameters are shown in Table.6.

The relationships of predicted values and actual values of the losses such as the electric machine loss, the inverter loss, and power difference between electromagnetic power and mechanical power using artificial neural network, k-nearest neighbors, decision tree, and random forest with the default parameters are illustrated in Fig.21, Fig.22, Fig.23, Fig.24, respectively.

Table.1 The default parameters of artificial neural network.

Hyperparameters	Default
Number of neurons	25
number of hidden layers	2
Epochs	100
Learning rate	0.001
Batch size	64

Table.2 The default parameters of k-nearest neighbors.

Hyperparameters	Default
Number of neighbors	5
Weight function	Uniform
Power parameter	2

Table.3 The default parameters of decision tree.

Hyperparameters	Default
n_estimators	10
max_depth	2
min_samples_split	1

Table.4 The default parameters of random forest.

Hyperparameters	Default
n_estimators	100
max_depth	10
min_samples_split	2

Table.5 Electrical parameter prediction results of artificial neural network (ANN), random forest (RF), decision tree (DT), k-nearest neighbors (kNN) with default parameters.

Model	Mean absolute percentage error			Mean squared error			R-squared score		
	Ud[%]	Uq[%]	Tq_el[%]	Ud[V]	Uq[V]	Tq_el[Nm]	Ud	Uq	Tq_el
ANN	4.99	10.65	2.88	0.49	0.39	1.58	0.99973	0.99833	0.99997
RF	1.45	30.45	1.28	0.13	0.39	11.86	0.99992	0.99844	0.99982
DT	2.02	16.02	1.45	0.42	0.80	22.50	0.99977	0.99676	0.99967
kNN	14.28	10.08	15.28	3.33	0.37	174	0.99821	0.99843	0.99751

Table.6 Loss prediction results of artificial neural network (ANN), random forest (RF), decision tree (DT), k-nearest neighbors (kNN) with default parameters

Model	Mean absolute percentage error			Mean squared error			R-squared score		
	Pmachine [%]	Pdiff [%]	Pinv [%]	Pmachine [W]	Pdiff [W]	Pinv [W]	Pmachine	Pdiff	Pinv
ANN	14.60	292.95	21.92	64409	393418	60471	0.99270	0.96395	0.96677
RF	4.94	108.95	5.57	45711	241530	7799	0.99482	0.97787	0.99571
DT	6.19	95.08	7.95	116482	367521	20239	0.98680	0.96633	0.98887
kNN	9.98	138.68	8.51	172110	697438	24343	0.98050	0.93610	0.98662



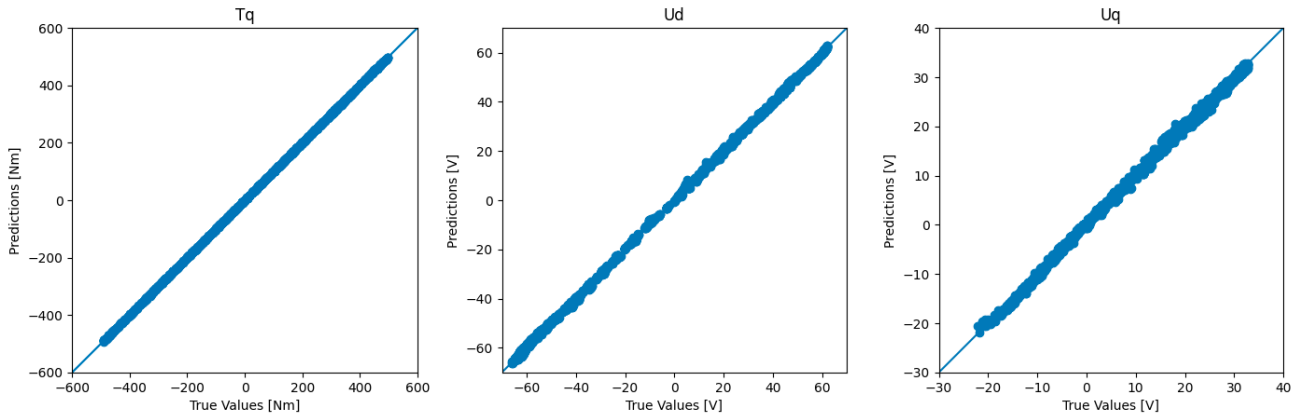


Fig.17 Relationships of predicted values and actual values of electromagnetic torque ( $T_q$ ), direct-axis voltage ( $U_d$ ), and quadrature-axis voltage ( $U_q$ ) using artificial neural network with default parameters.

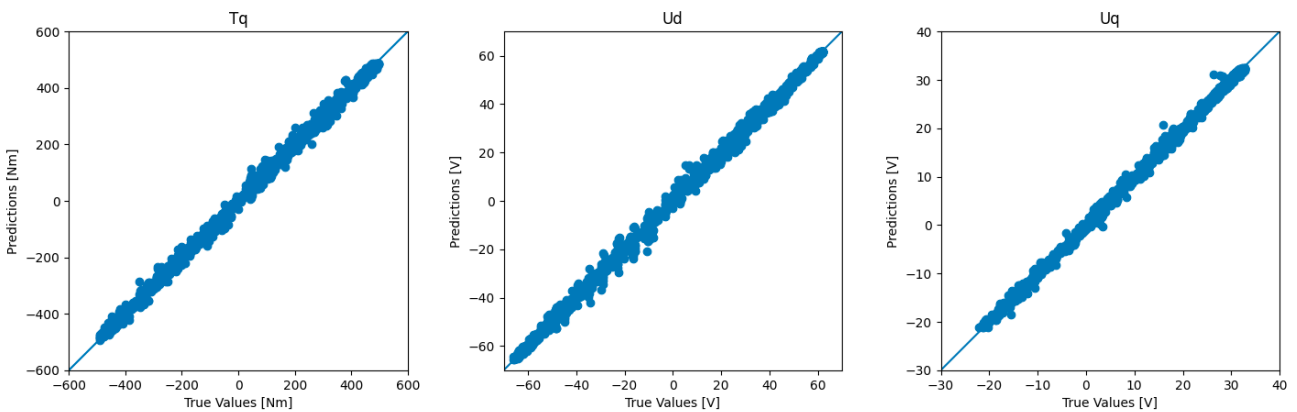


Fig.18 Relationships of predicted values and actual values of electromagnetic torque ( $T_q$ ), direct-axis voltage ( $U_d$ ), and quadrature-axis voltage ( $U_q$ ) using k-nearest neighbors with initial hyperparameters.

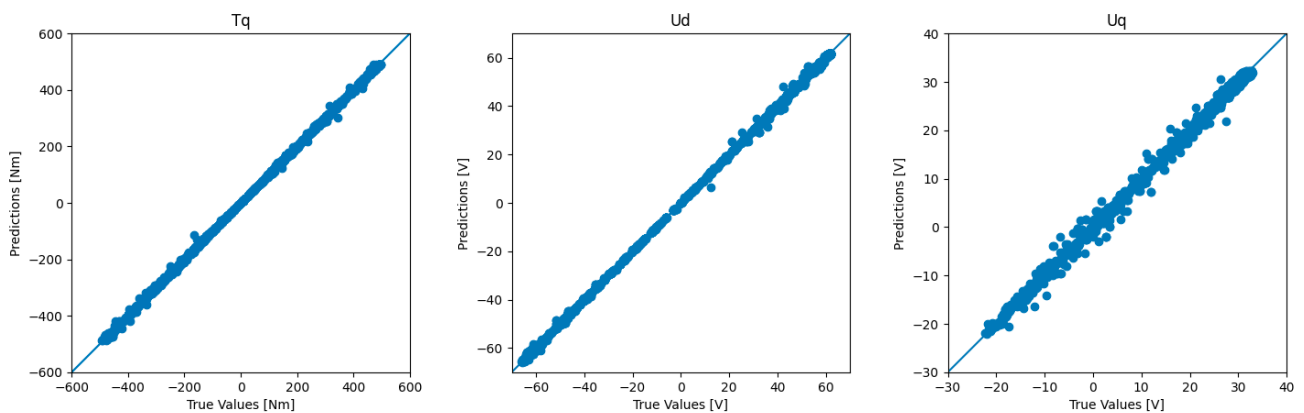


Fig.19 Relationships of predicted values and actual values of electromagnetic torque ( $T_q$ ), direct-axis voltage ( $U_d$ ), and quadrature-axis voltage ( $U_q$ ) using decision tree with initial hyperparameters.

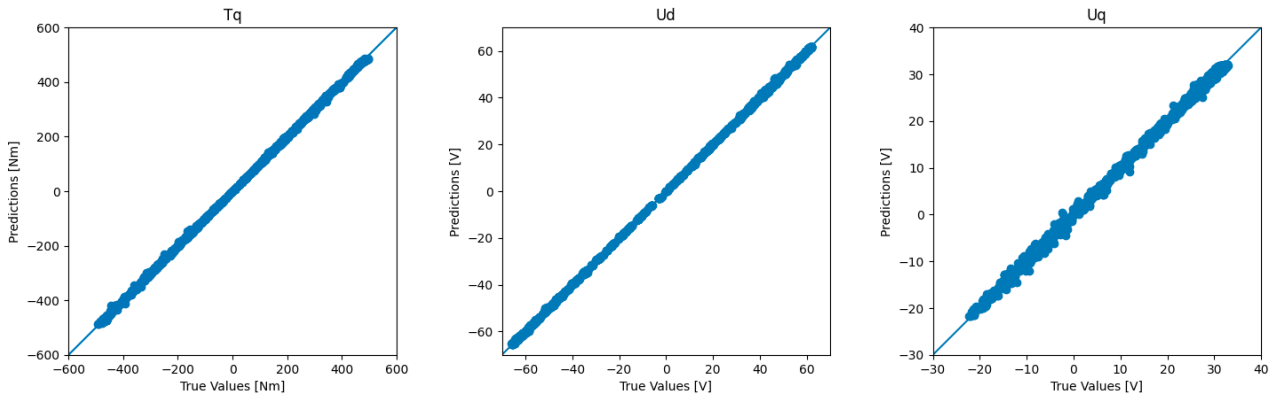


Fig.20 Relationships of predicted values and actual values of electromagnetic torque ( $T_q$ ), direct-axis voltage ( $U_d$ ), and quadrature-axis voltage ( $U_q$ ) using random forest with initial hyperparameters.

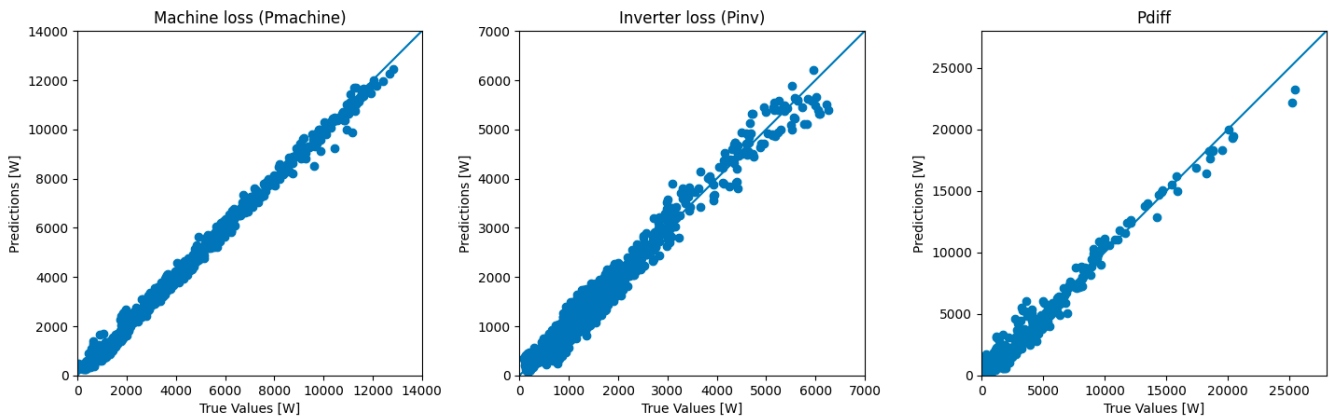


Fig.21 Relationships of predicted values and actual values of electric machine loss ( $P_{machine}$ ), inverter loss ( $P_{inv}$ ), and power difference between electromagnetic power and mechanical power ( $P_{diff}$ ) using artificial neural network with initial hyperparameters.

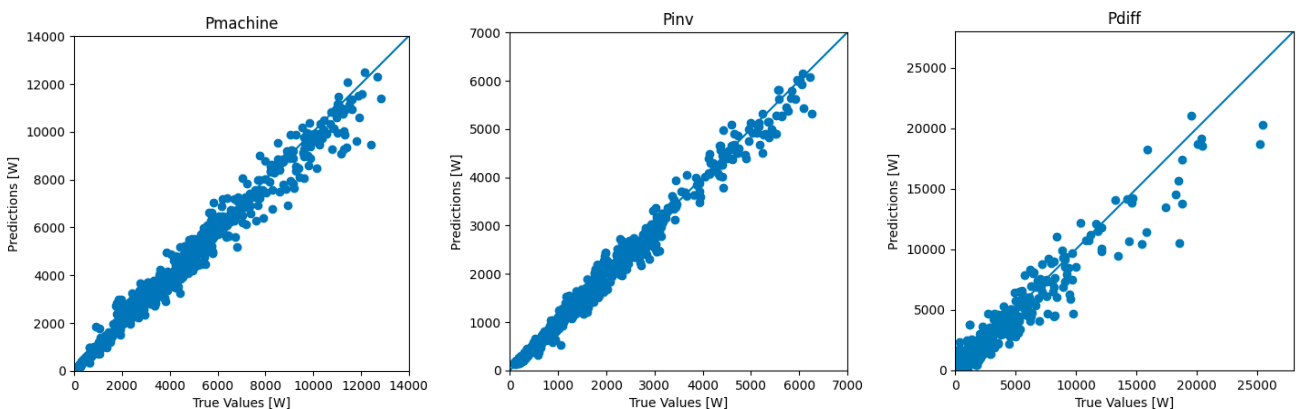


Fig.22 Relationships of predicted values and actual values of electric machine loss ( $P_{machine}$ ), inverter loss ( $P_{inv}$ ), and power difference between electromagnetic power and mechanical power ( $P_{diff}$ ) using k-nearest neighbors with initial hyperparameters.

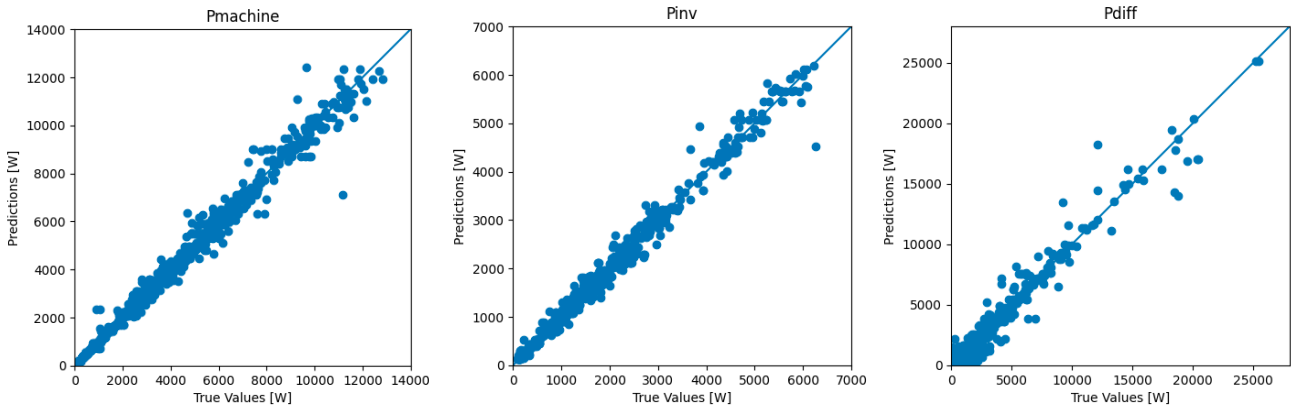


Fig.23 Relationships of predicted values and actual values of electric machine loss ( $P_{machine}$ ), inverter loss ( $P_{inv}$ ), and power difference between electromagnetic power and mechanical power ( $P_{diff}$ ) using decision tree with initial hyperparameters.

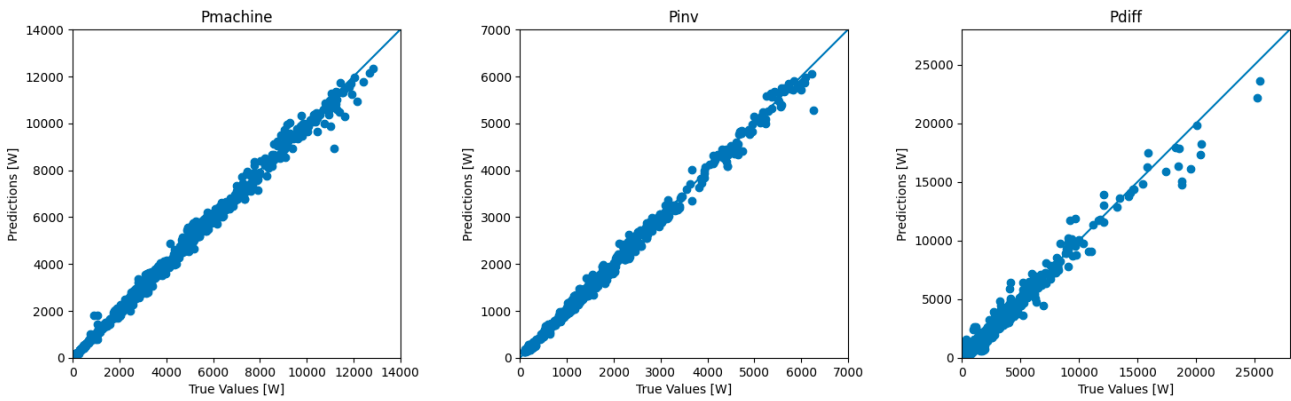


Fig.24 Relationships of predicted values and actual values of electric machine loss ( $P_{machine}$ ), inverter loss ( $P_{inv}$ ), and power difference between electromagnetic power and mechanical power ( $P_{diff}$ ) using random forest with initial hyperparameters.

## 5.2 Hyperparameter tuning

In this section, the prediction results of hyperparameter optimization in each prediction model are described. Grid search with 5-fold cross validation was implemented for hyperparameter tuning of each prediction model.

### 5.2.1 Hyperparameter tuning of artificial neural network

Some grid searches were conducted to optimize hyperparameters in artificial neural network. The conditions and the results of grid search are described in Table.7. The results of the electrical

parameter and loss prediction of neural network with initial and optimized hyperparameters are shown in Table.8 and Table.9, respectively.

Relationship of predicted values and true values of the electrical parameters and losses using artificial neural network with optimized hyperparameters are shown in Fig.25 and Fig.33 in section 5.3 and section 5.4.

Table.7 grid search conditions and the results of artificial neural network.

Hyperparameters	Grid search 1	Grid search 2	Grid search 3	Grid search 4	Grid search 5	Result
Number of neurons	[25, 50, 100]	[100, 200, 300, 400]	[400, 500, 600]	500	500	500
Number of hidden layers	2	[1, 2, 3]	[2, 3]	[3, 4, 5, 6]	4	4
Epochs	[50, 100, 200]	200	200	200	[200, 500, 1000, 1500, 1750, 2000]	1750
Learning rate	[0,01, 0.001, 0.0001]	0.001	0.001	0.001	0.001	0.001
Batch size	[16, 32, 64]	[32, 64, 128, 256]	64	64	64	64

Table.8 The electrical parameter prediction results of artificial neural network with optimized and initial hyperparameters.

Hyperparameters	Mean absolute percentage error			Mean squared error			R-squared score		
	Ud[%]	Uq[%]	Tq_el[%]	Ud[V]	Uq[V]	Tq_el[Nm]	Ud	Uq	Tq_el
Optimized	1.02	2.85	0.85	0.023	0.023	0.614	0.999987	0.999904	0.999991
Initial	4.99	10.65	2.88	0.489	0.395	1.579	0.999737	0.998336	0.999977

Table.9 The loss prediction results of artificial neural network with optimized and initial hyperparameters.

Hyperparameters	Mean absolute percentage error			Mean squared error			R-squared score		
	Pmachine [%]	Pdiff [%]	Pinv [%]	Pmachine [W]	Pdiff [W]	Pinv [W]	Pmachine	Pdiff	Pinv
Optimized	2.78	36.82	1.63	5259	41883	911	0.99940	0.99616	0.99950
Initial	14.60	292.95	21.92	64409	393418	60471	0.99270	0.96395	0.96677

## 5.2.2 Hyperparameter tuning of k-nearest neighbors

A grid search was executed to optimize hyperparameters in k-nearest neighbors regression. The conditions and the the results of grid search are shown in Table.10. The results of the electrical parameter and loss prediction of k-nearest neighbors with initial hyperparameters and optimized hyperparameters are shown in Table.11 and Table.12, respectively.

Relationship of predicted values and true values of the electrical parameters and losses using k-nearest neighbors with optimized hyperparameters are shown in Fig.31 and Fig.39, respectively, in section 5.3 and section 5.4.

Table.10 grid search conditions and the results of k-nearest neighbors regression.

Hyperparameters	Grid search	Result
Number of neighbors	[3, 5, 7, 10]	3
Weight function	[uniform, distance]	Distance
Power parameter	[1, 2]	2

Table.11 The electrical parameters prediction results of k-nearest neighbors with optimized and initial hyperparameters.

Hyperparameters	Mean absolute percentage error			Mean squared error			R-squared score		
	Ud[%]	Uq[%]	Tq_el[%]	Ud[V]	Uq[V]	Tq_el[Nm]	Ud	Uq	Tq_el
Optimized	16.86	9.86	13.57	3.14	0.29	161	0.998313	0.998778	0.997706
Initial	14.28	10.08	15.28	3.33	0.37	174	0.998212	0.998437	0.997512

Table.12 The loss prediction results of k-nearest neighbors with optimized and initial hyperparameters.

Hyperparameters	Mean absolute percentage error			Mean squared error			R-squared score		
	Pmachine [%]	Pdiff [%]	Pinv [%]	Pmachine [W]	Pdiff [W]	Pinv [W]	Pmachine	Pdiff	Pinv
Optimized	8.07	107.57	7.18	101059	537183	16041	0.98855	0.95079	0.99119
Initial	9.98	138.68	8.51	172110	697438	24343	0.98050	0.93610	0.98662

### 5.2.3 Hyperparameter tuning of decision tree

To adjust hyperparameters in decision tree regression model, a grid search was implemented. The conditions and the results of grid search are shown in Table.13. The results of the electrical parameter and loss prediction of decision tree with initial hyperparameters and optimized hyperparameters are shown in Table.14 and Table.15, respectively.

Relationship of predicted values and true values of the electrical parameters and losses using decision tree with optimized hyperparameters are shown in Fig.30 and Fig.38, respectively, in section 5.3 and section 5.4.

Table.13 grid search conditions and the results of decision tree regression.

Hyperparameters	Grid search	Result
max_depth	[5, 10, 20, 30, 50, 70, 90, 100]	50
min_samples_split	[2, 5, 10]	2
min_samples_leaf	[1, 2, 4]	1

Table.14 The electrical parameters prediction results of decision tree with optimized and initial hyperparameters

Hyperparameters	Mean absolute percentage error			Mean squared error			R-squared score		
	Ud[%]	Uq[%]	Tq_el[%]	Ud[V]	Uq[V]	Tq_el[Nm]	Ud	Uq	Tq_el
Optimized	1.39	7.08	0.80	0.22	0.52	13.01	0.999880	0.997907	0.999810
Initial	2.02	16.02	1.45	0.42	0.80	22.50	0.999773	0.996766	0.999671

Table.15 The loss prediction results of decision tree with optimized and initial hyperparameters

Hyperparameters	Mean absolute percentage error			Mean squared error			R-squared score		
	Pmachine [%]	Pdiff [%]	Pinv [%]	Pmachine [W]	Pdiff [W]	Pinv [W]	Pmachine	Pdiff	Pinv
Optimized	4.97	82.16	5.22	103535	310317	16510	0.98827	0.97157	0.99093
Initial	6.19	95.08	7.95	116482	367521	20239	0.98680	0.96633	0.98887

## 5.2.4 Hyperparameter tuning of random forest

A grid search was conducted to optimize random forest regression model's hyperpartameters. The conditions and the the results of grid search are shown in Table.16. The results of the electrical parameter and loss prediction of random forest with initial and optimized hyperparameters are shown in Table.17 and Table.18, respectively.

Relationship of predicted values and true values of the electrical parameters and losses using random forest with optimized hyperparameters are shown in Fig.29 and Fig.37, respectively, in section 5.3 and 5.4.

Table.16 grid search conditions and the results of random forest regression.

Hyperparameters	Grid search	Result
n_estimators	[100, 200, 300, 400, 500, 600, 700]	600
max_depth	[5, 10, 15, 30, 45, 60, 90]	60
min_samples_split	[2, 5, 10]	2
max_features	['sqrt', 'log2', None]	None

Table.17 The electrical parameters prediction results of random forest with optimized and initial hyperparameters.

Hyperparameters	Mean absolute percentage error			Mean squared error			R-squared score		
	Ud[%]	Uq[%]	Tq_el[%]	Ud[V]	Uq[V]	Tq_el[Nm]	Ud	Uq	Tq_el
Optimized	1.12	8.40	0.90	0.0499	0.150	7.111	0.999973	0.999395	0.999896
Initial	1.45	30.45	1.28	0.1318	0.388	11.856	0.999929	0.998440	0.999827

Table.18 The loss prediction results of random forest with optimized and initial hyperparameters.

Hyperparameters	Mean absolute percentage error			Mean squared error			R-squared score		
	Pmachine [%]	Pdiff [%]	Pinv [%]	Pmachine [W]	Pdiff [W]	Pinv [W]	Pmachine	Pdiff	Pinv
Optimized	4.25	87.55	3.88	39462	219553	5173	0.99553	0.97989	0.99716
Initial	4.94	108.95	5.57	45711	241530	7799	0.99482	0.97787	0.99571

## 5.3 Electrical parameter predictions

In this section, prediction results of electric parameters including electromagnetic torque, d-axis voltage, and q-axis voltage using artificial neural network, random forest, decision tree, k-nearest neighbors are explained.

### 5.3.1 Artificial neural network

An artificial neural network model with hyperparameters optimized by grid search was trained using the training data set. The mean squared error (MSE) and mean absolute percentage error (MAPE)

and coefficient of determination ( $R^2$ ) of prediction of the neural network model are illustrated in Table.19. The relationship between predicted values and actual values of electromagnetic torque, d-axis voltage, and q-axis voltage are shown in Fig.25.

The residual plots of electromagnetic torque, d-axis voltage, and q-axis voltage are shown in Fig.26, Fig.27, and Fig.28, respectively.

Regarding electromagnetic torque and d-axis voltage, the error percentage was less than 1 % except for around 0 [Nm] and 0 [V]. When it comes to q-axis voltage, the error percentage was less than 5 % other than around 0 [V]. The closer the true value is to 0 [Nm] and 0 [V], the larger the error, because division by values near 0 makes the percentage error ratio worse, even if the actual error is approximately equal to the other value ranges of the true value. As for actual differences between true values and predicted values, the maximum absolute difference of electromagnetic torque was less than 3.5 [Nm], the maximum absolute difference of d-axis voltage and q-axis voltage were less than 0.5 [V].

In the research of He et al. (2022), the accuracy of the artificial neural network for the electromagnetic torque prediction shows 95%. Yan et al. (2019) also developed a neural network model to predict electromagnetic torque and the model performed 98.3% accuracy. The artificial neural network model developed by Nawae and Thongpull (2020) performed the best with R-squared score of 0.996 compared with the other models including linear regression, stepwise regression.

Compared to these models of their research, the artificial neural network model of this project produced better results, with a MAPE of more than 99% and an R-squared score of more than 0.999, although the quality of the dataset and the input variables are different.

Table.19 Prediction results of artificial neural network model.

Model	Mean absolute percentage error			Mean squared error			R-squared score		
	Ud[%]	Uq[%]	Tq_el[%]	Ud[V]	Uq[V]	Tq_el[Nm]	Ud	Uq	Tq_el
ANN	1.02	2.85	0.85	0.023	0.023	0.614	0.999987	0.999904	0.999991



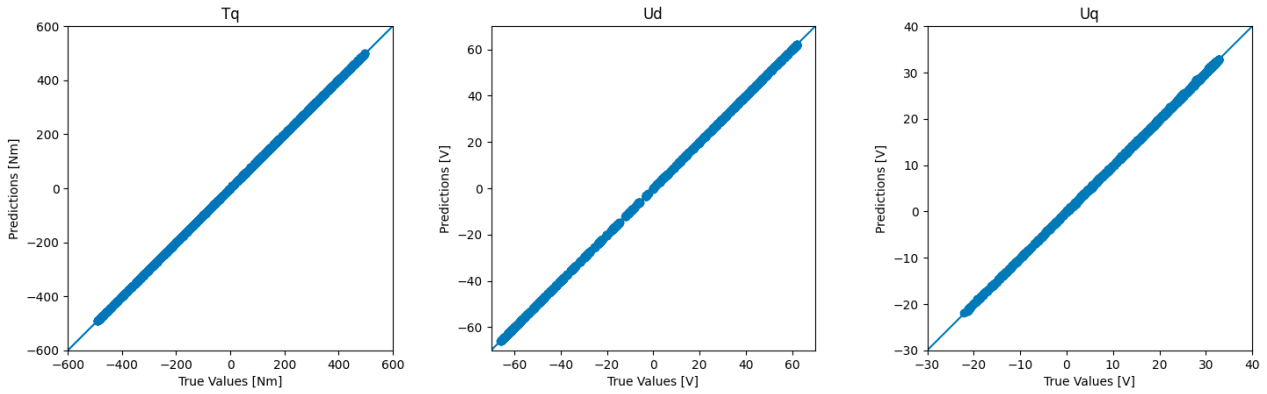


Fig.25 Relationship of predicted values and actual values of electromagnetic torque ( $T_q$ ), direct-axis voltage ( $U_d$ ), and quadrature-axis voltage ( $U_q$ ).

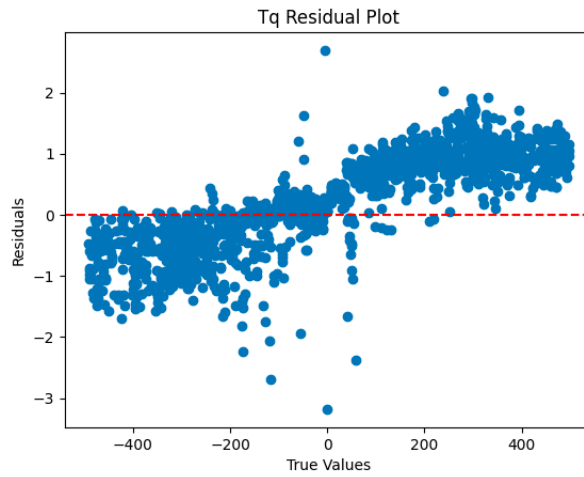


Fig.26 Residual plot of electromagnetic torque.

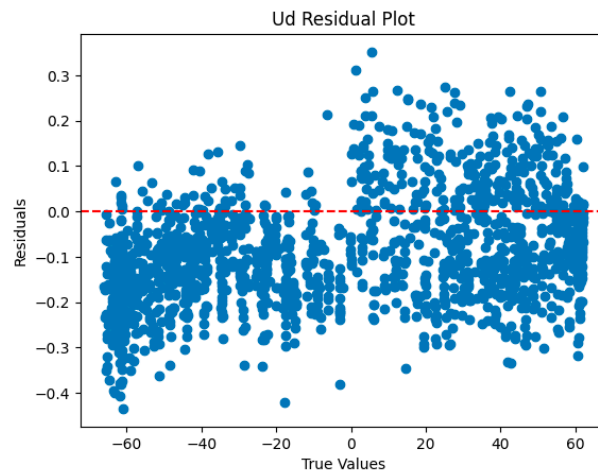


Fig.27 Residual plot of direct-axis voltage.

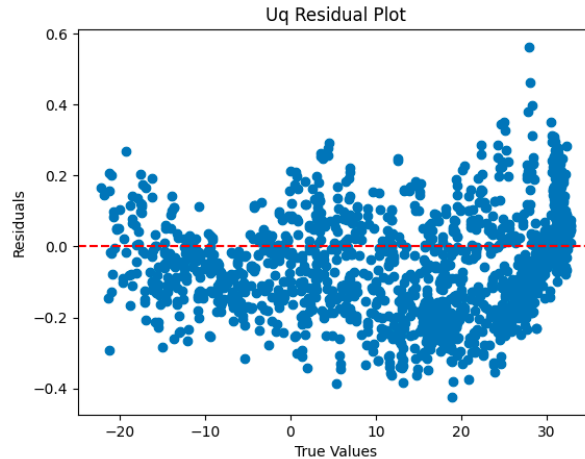


Fig.28 Residual plot of quadrature-axis voltage.

### 5.3.2 Other machine learning models

The hyperparameters adjusted by grid search were used to train each model. The mean squared error (MSE) and mean absolute percentage error (MAPE) and coefficient of determination ( $R^2$ ) of artificial neural network, other prediction models, such as k-nearest neighbors, decision tree, random forest, and multiple linear regression with a quadratic model results are shown in Table.20. The relationship between predicted values and true values of electromagnetic torque, d-axis voltage, and q-axis voltage in random forest, decision tree, k-nearest neighbors, and multiple linear regression with a quadratic model are illustrated in Fig.29, Fig.30, Fig.31, and Fig.32, respectively.

When the artificial neural network results were compared to other machine learning results, artificial neural network produced better results for each target variable in MSE, R-squared scores, and MAPE than the other machine learning algorithms. The results indicate that artificial neural network has advantages to handle complex non-linear relationships like electric system.

Among the other three machine learning algorithms, the random forest model showed the best performance in MSE and R-squared score for all the predicted variables, which was followed by the decision tree except for q-axis voltage prediction. The k-nearest neighbors performed the much worse for predicting d-axis voltage and electromagnetic torque than random forest and decision tree because the k-nearest neighbors simply choose the nearest point as the predicted outputs so it was difficult to predict complex relationship in electric system. However it got better results in MSE and

R-squared score for predicting q-axis voltage. Random forest performed better than decision tree because random forest ensembles decision trees and takes average of them as predicted values. Multiple linear regression with a quadratic model produced the worst forecasting results because the relationships between the inputs and outputs had more intricate nonlinearities than a quadratic relationship, which made it difficult to model.

Additionally, looking at the graphs of the relationship between predicted values and true values, it is visually understandable that the machine learning results such as random forest, decision tree, and k-nearest neighbors have larger deviations from the actual values in comparison with the prediction results of artificial neural network.

Table.20 Prediction results of artificial neural network (ANN), random forest (RF), decision tree (DT), k-nearest neighbors (kNN), and multiple linear regression with a quadratic model (MLR).

Model	Mean absolute percentage error			Mean squared error			R-squared score		
	Ud[%]	Uq[%]	Tq_el[%]	Ud[V]	Uq[V]	Tq_el[Nm]	Ud	Uq	Tq_el
ANN	1.02	2.85	0.858	0.023	0.023	0.614	0.999987	0.999904	0.999991
RF	1.12	8.40	0.900	0.050	0.150	7.111	0.999973	0.999395	0.999896
DT	1.39	7.08	0.796	0.221	0.520	13.006	0.999880	0.997907	0.999810
kNN	16.86	9.86	13.571	3.135	0.290	160.627	0.998313	0.998778	0.997706
MLR	31.17	95.34	15.385	66.521	1.580	778.382	0.964001	0.993651	0.988644

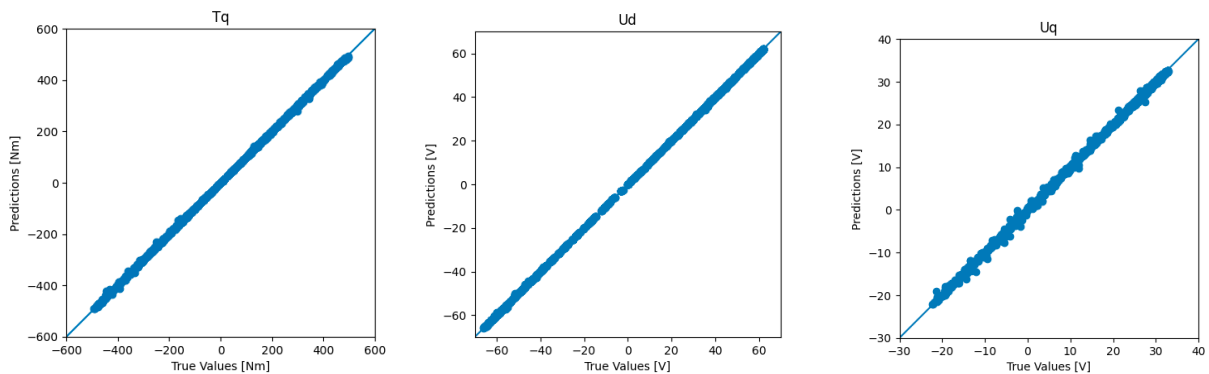


Fig.29 Relationship between predicted values and actual values of electromagnetic torque (Tq), direct-axis voltage (Ud), and quadrature-axis voltage (Uq) in random forest.

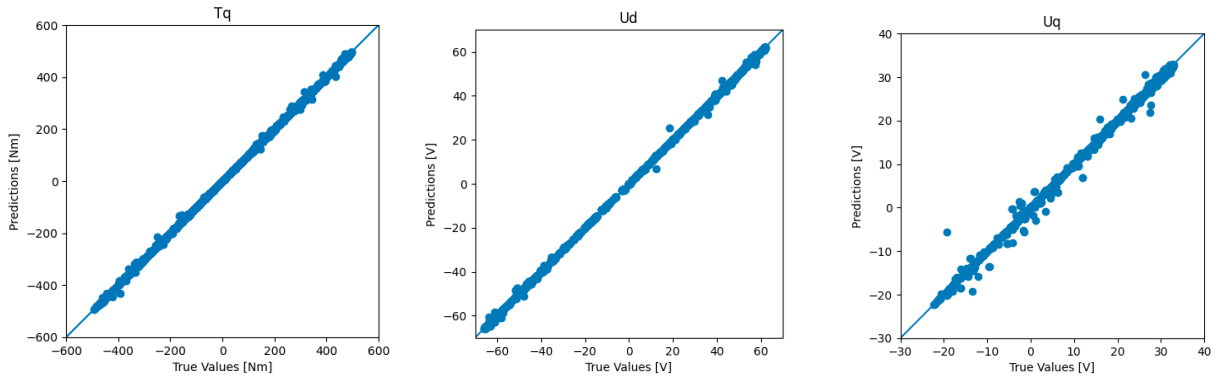


Fig.30 Relationship between predicted values and actual values of electromagnetic torque ( $T_q$ ), direct-axis voltage ( $U_d$ ), and quadrature-axis voltage ( $U_q$ ) in decision tree.

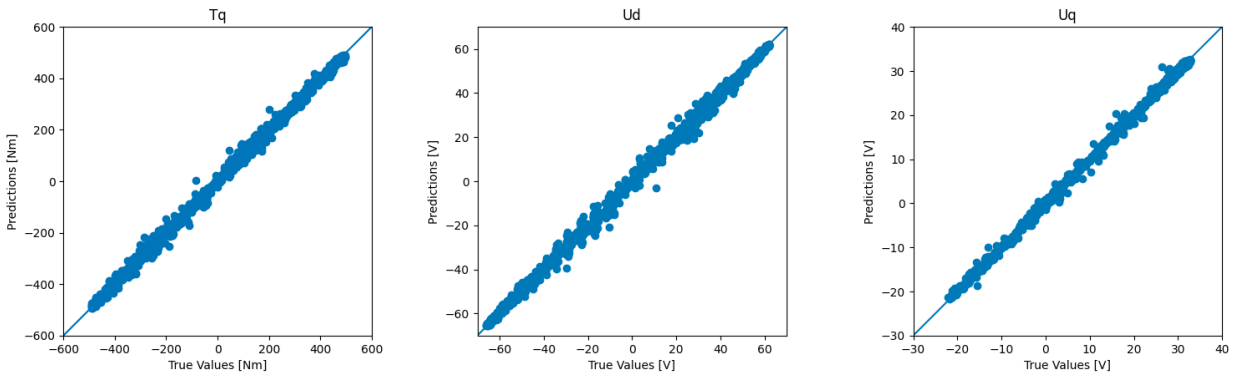


Fig.31 Relationship between predicted values and actual values of electromagnetic torque ( $T_q$ ), direct-axis voltage ( $U_d$ ), and quadrature-axis voltage ( $U_q$ ) in k-nearest neighbors.

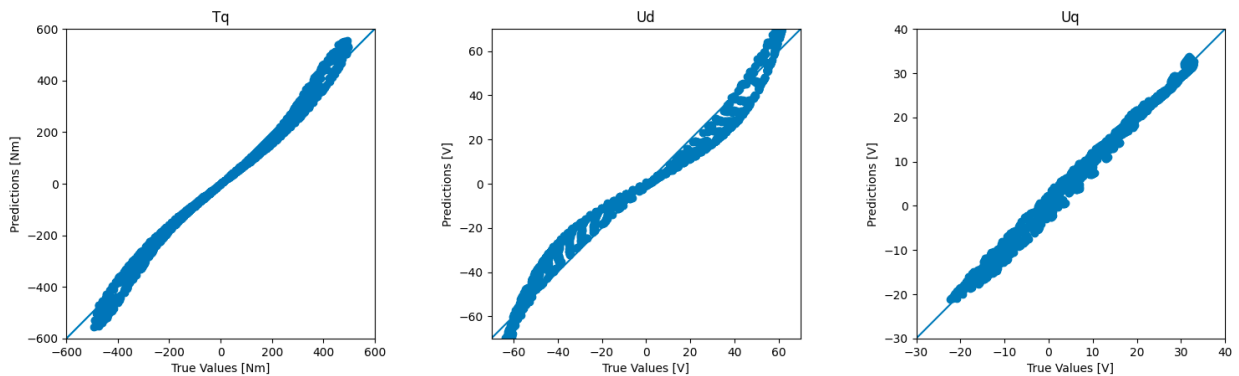


Fig.32 Relationship between predicted values and actual values of electromagnetic torque ( $T_q$ ), direct-axis voltage ( $U_d$ ), and quadrature-axis voltage ( $U_q$ ) in multiple linear regression with a quadratic model.

## 5.4 Loss predictions

In this section, prediction results of losses such as total machine loss and inverter loss by three-output neural network, one-output neural network, random forest, decision tree, k-nearest neighbors are described.

### 5.4.1 Artificial neural network

A neural network model that has hyperparameters optimized by grid search was trained using the training dataset. The mean squared error (MSE) and the mean absolute percentage error (MAPE) and coefficient of determination ( $R^2$ ) of prediction results of the neural network model are shown in Table.21. The relationship between predicted values and actual values of the electric machine loss, the inverter loss, and the power difference between electromagnetic power and mechanical power are shown in Fig.33. The residual plots of the electric machine loss, the inverter loss, and the power difference between electromagnetic power and mechanical power are depicted in Fig.34, Fig.35, and Fig.36, respectively.

Regarding the electric machine loss, the error percentages were less than 10 % when the loss was greater than 4000[W] and the error percentages were less than 20 % when the loss was greater than 2000[W]. The error percentage shows less than 5% when the loss is greater than 6000 [W]. When it comes to the inverter loss, the error percentages were less than 10 % when the loss was greater than 500 [W] and less than 5 % when the loss was greater than 3500 [W] at almost all points. For the power difference between electromagnetic power and mechanical power, the error rates were less than 10 % when the loss was greater than 5000 [W] and less than 5 % when the loss was greater than 9000 [W] at almost all points. The closer the true value is to 0 [W], the larger the percentage error, because division by values near 0 makes the percentage error ratio worse, even if the actual error is approximately equal to the other value ranges of the true value. MAPE of the power difference is much larger than other losses because the power difference have much more data around 0 [W].

As for actual differences between true values and predicted values, the maximum difference of the electric machine loss was less than 600 [W], the maximum difference of the inverter loss was less than 400 [W], and the maximum error of the power difference between electromagnetic power and mechanical power was less than 2500 [W]. Almost all the errors of the power difference are less than 800 [W] when the true value is greater than 5500 [W].

He et al. (2022) developed neural network to predict the rotor core loss and stator core loss with the error of 14 % and 20 %, respectively. The neural network of this project anticipates total electric machine loss, therefore, it is difficult to compare the results directly, however, the MAPE of the electric machine showed around 2.8% which is much lower than the errors of the losses predicted by the neural network model built by He et al. (2022).

Table.21 Prediction results of artificial neural network.

Model	Mean absolute percentage error			Mean squared error			R-squared score		
	Pmachine [%]	Pdiff [%]	Pinv [%]	Pmachine [W]	Pdiff [W]	Pinv [W]	Pmachine	Pdiff	Pinv
ANN	2.78	36.82	1.63	5259	41883	911	0.99940	0.99616	0.99950

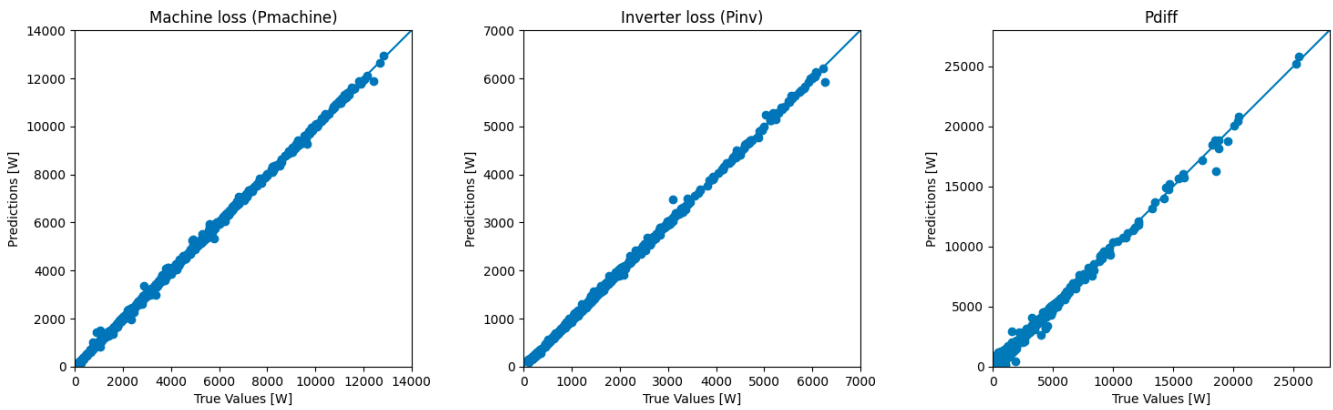


Fig.33 Relationship of predicted values and actual values of electric machine loss (Pmachine), inverter loss (Pinv), and power difference between electromagnetic power and mechanical power (Pdiff).

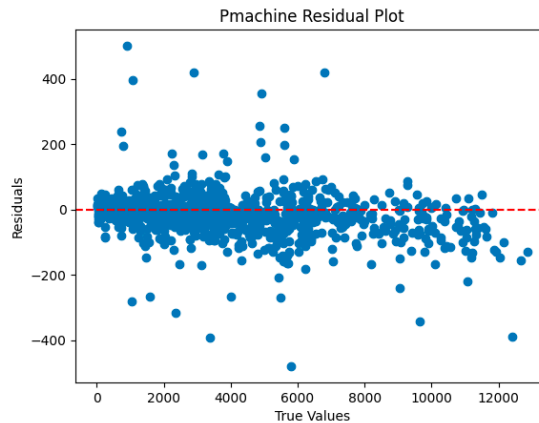


Fig.34 Residual plot of the electric machine loss.

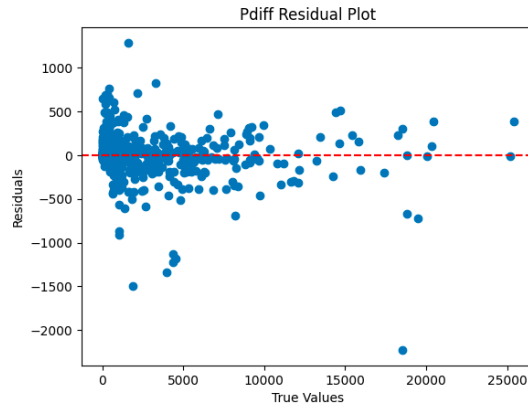


Fig.35 Residual plot of the inverter loss.

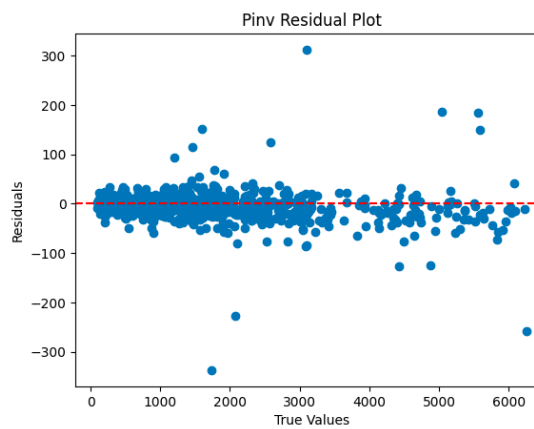


Fig.36 Residual plot of power difference between electromagnetic power and mechanical power.

## 5.4.2 Other machine learning models

The hyperparameters tuned by grid search were used to train each machine learning model including k-nearest neighbors, decision tree, random forest, and multiple linear regression with a quadratic model. The MSE, R-squared score, and MAPE of each machine learning prediction results are shown in Table.22. The relationship between predicted values and true values of the electric machine loss, the inverter loss, and the power difference between electromagnetic power and mechanical power in random forest, decision tree, k-nearest neighbors, and multiple linear regression with a quadratic model are depicted in Fig.37, Fig.38, Fig.39, and Fig.40, respectively.

When the artificial neural network results were compared with those of other machine learning models, artificial neural network outperformed the other machine learning algorithms in MSE, R-

squared score, and MAPE for each target variable. The results indicate that artificial neural network has advantages to handle complex non-linear relationships like electric system.

Among other machine learning algorithms, the random forest model showed the best performance in MSE and R-squared score for all the predicted variables, which is followed by decision tree for predicting the power difference between electromagnetic power and mechanical power, and multiple linear regression with a quadratic model for the prediction of the electric machine loss and the inverter loss. The k-nearest neighbors and decision tree generated similar results in MSE and R-squared score for the electric machine loss and the inverter loss, which was the worst. The random forest performed better than the decision tree because the random forest ensembles hundreds of decision trees and takes average of them as predicted values. The k-nearest neighbors merely select the nearest point as the predicted outputs so it was difficult to predict complex relationship. The multiple linear regression with a quadratic model performed the worst for anticipating the power difference between electromagnetic power and mechanical power because the relationship between input and output variables was too complicated to handle with a multiple quadratic equation. The graphs of the relationships between predictions and true values also provides a visual understanding that machine learning results such as random forests, decision trees, and k-nearest neighbors deviate more from the true values than the prediction results of artificial neural networks.

Table.22 Prediction results of each model.

Model	Mean absolute percentage error			Mean squared error			R-squared score		
	Pmachine [%]	Pdiff [%]	Pinv [%]	Pmachine [W]	Pdiff [W]	Pinv [W]	Pmachine	Pdiff	Pinv
ANN	2.78	36.82	1.63	5259	41883	911	0.99940	0.99616	0.99950
RF	4.25	87.55	3.88	39462	219553	5173	0.99553	0.97989	0.99716
DT	4.97	82.16	5.22	103535	310317	16510	0.98827	0.97157	0.99093
kNN	8.07	107.57	7.18	101059	537183	16041	0.98855	0.95079	0.99119
MLR	28.19	1180.71	12.92	50874	1445137	15925	0.99423	0.86761	0.99124



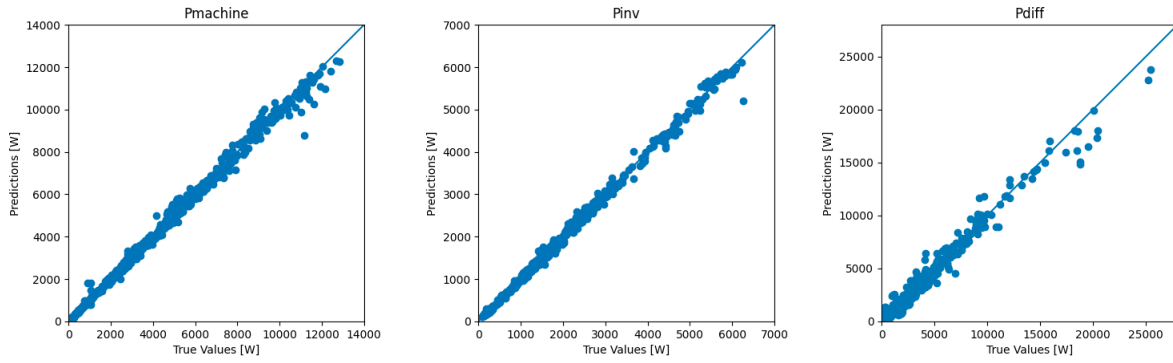


Fig.37 Relationship between predicted values and actual values of electric machine loss ( $P_{machine}$ ), inverter loss ( $P_{inv}$ ), and power difference between electromagnetic power and mechanical power ( $P_{diff}$ ) in random forest.

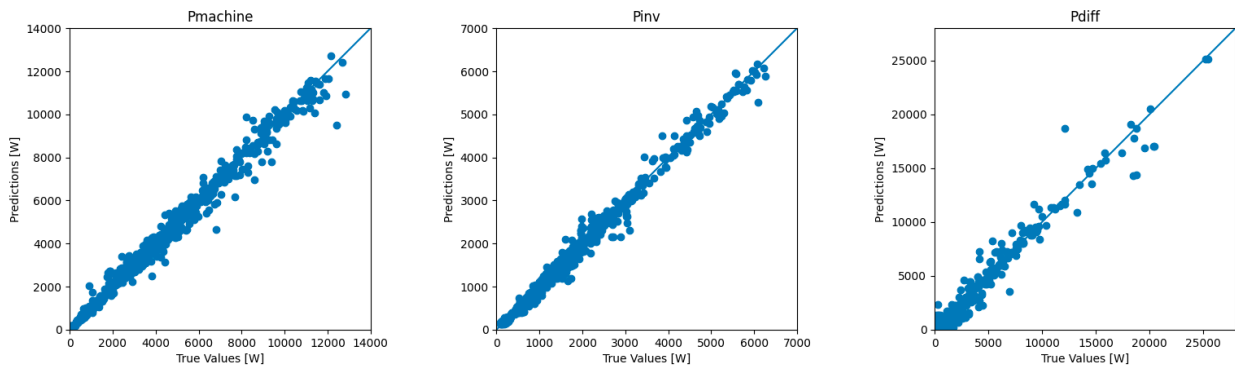


Fig.38 Relationship between predicted values and actual values of electric machine loss ( $P_{machine}$ ), inverter loss ( $P_{inv}$ ), and power difference between electromagnetic power and mechanical power ( $P_{diff}$ ) in decision tree.

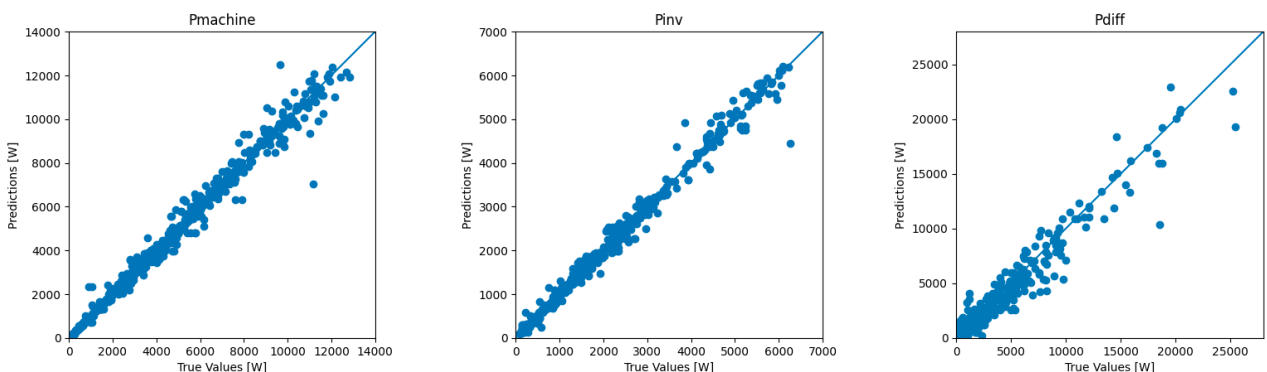


Fig.39 Relationship between predicted values and actual values of electric machine loss ( $P_{machine}$ ), inverter loss ( $P_{inv}$ ), and power difference between electromagnetic power and mechanical power ( $P_{diff}$ ) in k-nearest neighbors.

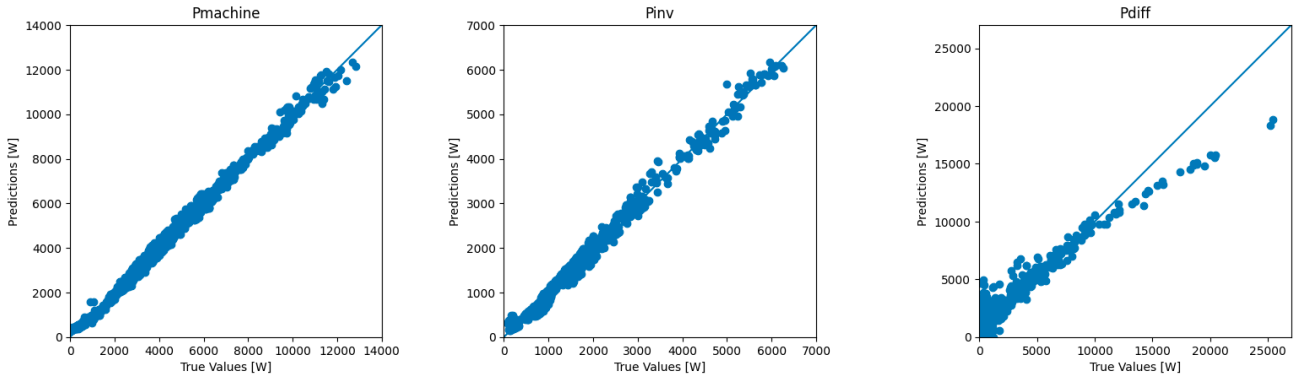


Fig.40 Relationship between predicted values and actual values of electric machine loss ( $P_{machine}$ ), inverter loss ( $P_{inv}$ ), and power difference between electromagnetic power and mechanical power ( $P_{diff}$ ) in multiple linear regression with a quadratic model.

## 6. Conclusions and Future Work

The summary and discussion of the results are conducted in this chapter. In addition, sustainability and ethics are discussed in the following part. Suggestions about future work are also described in the last part.

### 6.1 Summary of result

The artificial neural network and machine learning models are developed to predict electrical parameters and losses as new prediction approaches for the performance of Volvo Cars' electric vehicle. The electrical parameters includes electromagnetic torque, d-axis voltage, and q-axis voltage and the losses contains the electric machine loss, the inverter loss, and the power difference between electromagnetic power and mechanical power.

For objective1, the input and output data for each prediction model were extracted and calculated from the test operation database of Volvo Cars Corporation. The input data was normalized to smooth the impact of each input variable. Moreover, the correlation matrices of the normalized input were created and they indicated that the rotor temperature and the winding resistance have a high correlation in the electrical parameter prediction dataset. In addition, they showed that the rotor temperature and the winding temperature have a high correlation in the loss prediction dataset. Those are because the temperatures are similar due to their high thermal conductivity and the winding resistance is related to the winding temperature. The principle component analyses were also conducted.

For objective2 and 3, the artificial neural network and other machine learning models including k-nearest neighbors, decision tree regression, and random forest regression and multiple linear regression with a quadratic model are developed to predict electrical parameters and losses of EV and their hyperparameters were optimized by grid search with 5-fold cross validation to improve the accuracy of the prediction models.

For objective4, the evaluations of the prediction results of each model were conducted. For all parameters and loss predictions, the artificial neural networks performed the best in MSE and R-squared scores. The results indicate that artificial neural network are advantageous in dealing with complex nonlinear relationships such as electric system in comparison with other machine learning algorithms. Random forest showed better result than other machine leaning algorithms such as

decision tree, k-nearest neighbors, and multiple linear regression with a quadratic model. As for parameter prediction, the decision tree model produced better prediction results in MSE and R-squared score than k-nearest neighbors model except for q-axis voltage. Multiple linear regression with a quadratic model produced the worst results for the electric parameters prediction because the relationship between the input and output was too intricate to handle with a multiple quadratic equation. Decision tree produced worse results than random forest because random forest ensemble hundreds of subset of decision trees and averaging the results. K-nearest neighbors performed worse than decision tree for almost all the electrical parameters prediction because it merely selects the nearest points and utilizes the average as the predicted outputs so it was difficult to predict complex non-linear relationship like electrical systems. However, it is useful for dealing with simple relationships and gaining insight into relationships in data. For loss prediction, the k-nearest neighbors and decision tree produced similar results in MSE and R-squared score for the electric machine loss and the inverter loss, which was worse than the multiple linear regression with a quadratic model. However, they performed better than the multiple linear regression with a quadratic model for forecasting the power difference between electromagnetic power and mechanical power.

## **6.2 Contribution to sustainability**

Electric vehicle energy efficiency can be increased by optimizing motor control strategies as a result of accurate electrical parameters and loss prediction. By reducing energy consumption, the project supports in the conservation of important natural resources, promoting environmental sustainability.

Compared to conventional vehicles driven by internal combustion engines, electric vehicles have the potential to drastically reduce carbon emissions. The project indirectly helps to lower air pollution, mitigate climate change, and preserve the environment by enhancing the efficiency and performance of PMSMs through accurate electrical parameter and loss prediction.

The improvement of motor performance and reliability may result from the creation of sophisticated prediction models for PMSMs. The lifetime and dependability of electric vehicle powertrains can be ensured by precisely predicting parameters and losses, which also enables the early detection and proactive treatment of potential problems and failures. This benefits the economy by lowering maintenance costs and raising the satisfaction of consumers.

It can also lead to cost reduction in manufacturing and operation. Electric vehicles become more accessible and more widely used as a result of lower production costs, which also promote their adoption. By offering easily accessible and sustainable mobility solutions, it contributes to social and economic development.

### **6.3 Ethics**

Data security and privacy issues may arise from the use of test operation data from Volvo Cars Corporation. The data may contain private information that could be misused and have detrimental effects on the organization. While retaining the highest level of transparency for scholarly purposes, attention has been taken not to reveal anything that would harm the company. Before utilizing the company's test operation data, a clear confidentiality agreement was established with the company. Furthermore, solid information handling methods, such as secure storage, access controls, and anonymizing techniques, are implemented to protect the confidentiality of the company's data.

### **6.4 Future work**

By collecting data under more diverse conditions, a more versatile model can be developed. For example, if data at a wider range of temperatures and shaft rotation speed is collected, models that have more generality for the variation of temperature and shaft rotation speed could be developed. Also, if the artificial neural network model for the electrical parameter prediction train with test data performed at wider range of shaft rotation speed, the prediction results of electromagnetic torque using the dataset with 1000 rpm to 14000 rpm can become more appropriate so that the value of power difference between electromagnetic power and mechanical power in loss prediction can be more proper.

Several hyperparameters were adjusted to improve the artificial neural network and machine learning models in this research. This could be turned into a more extensive parameter tuning to further improve the results although the process would take longer time when tuning more hyperparameters.

Moreover, developing artificial neural networks for other models of electric machine is useful to predict each machine model's electrical parameters and losses because each machine has edifferent characteristics.

In addition, statistical methods are also be able to utilized to predict the electrical parameters and losses and compare the performance with artificial neural networking machine learning models.

## References

- An, X., Liu, G., Chen, Q., Zhao, W., & Song, X. (2021). Adjustable model predictive control for IPMSM drives based on online stator inductance identification. *IEEE Transactions on Industrial Electronics*, 69(4), 3368-3381.
- Badillo, S., Banfai, B., Birzele, F., Davydov, I. I., Hutchinson, L., Kam-Thong, T., ... & Zhang, J. D. (2020). An introduction to machine learning. *Clinical pharmacology & therapeutics*, 107(4), 871-885.
- Bel, L., Allard, D., Laurent, J. M., Cheddadi, R., & Bar-Hen, A. (2009). CART algorithm for spatial data: Application to environmental and ecological data. *Computational Statistics & Data Analysis*, 53(8), 3082-3093.
- Bingi, K., Prusty, B. R., Kumra, A., & Chawla, A. (2021, March). Torque and temperature prediction for permanent magnet synchronous motor using neural networks. In *2020 3rd International Conference on Energy, Power and Environment: Towards Clean Energy Technologies* (pp. 1-6). IEEE.
- Bishop, Christopher M., and Nasser M. Nasrabadi. *Pattern recognition and machine learning*. Vol. 4. No. 4. New York: springer, 2006.
- Chiu, C. C., Sainath, T. N., Wu, Y., Prabhavalkar, R., Nguyen, P., Chen, Z., ... & Bacchiani, M. (2018, April). State-of-the-art speech recognition with sequence-to-sequence models. In *2018 IEEE international conference on acoustics, speech and signal processing (ICASSP)* (pp.4774-4778). IEEE.
- Breiman, L. (2001). Random forests. *Machine learning*, 45, 5-32.
- Cappugi, L., Castorrini, A., Bonfiglioli, A., Minisci, E., & Campobasso, M. S. (2021). Machine learning-enabled prediction of wind turbine energy yield losses due to general blade leading edge erosion. *Energy Conversion and Management*, 245, 114567.
- Clark, K., Vendt, B., Smith, K., Freymann, J., Kirby, J., Koppel, P., ... & Prior, F. (2013). The Cancer Imaging Archive (TCIA): maintaining and operating a public information repository. *Journal of digital imaging*, 26(6), 1045-1057.
- Fujiyoshi, H., Hirakawa, T., & Yamashita, T. (2019). Deep learning-based image recognition for autonomous driving. *IATSS research*, 43(4), 244-252.
- Gou, J., Du, L., Zhang, Y., & Xiong, T. (2012). A new distance-weighted k-nearest neighbor classifier. *J. Inf. Comput. Sci*, 9(6), 1429-1436.
- Guo, H., Ding, Q., Song, Y., Tang, H., Wang, L., & Zhao, J. (2020). Predicting temperature of permanent magnet synchronous motor based on deep neural network. *Energies*, 13(18), 4782.
- Han, J., Kamber, M., & Pei, J. (2012). *Data mining concepts and techniques third edition*. University of Illinois at Urbana-Champaign Micheline Kamber Jian Pei Simon Fraser University.

- He, L., Wu, X., Nie, Y., & Shi, W. (2022). Loss Prediction of Vehicle Permanent Magnet Synchronous Motor Based on Deep Learning. *Journal of Electrical Engineering & Technology*, 1-11.
- Kaelbling, L. P., Littman, M. L., & Moore, A. W. (1996). Reinforcement learning: A survey. *Journal of artificial intelligence research*, 4, 237-285.
- Koçak, Y., & Şiray, G. Ü. (2021). New activation functions for single layer feedforward neural network. *Expert systems with applications*, 164, 113977.
- Liashchynskiy, P., & Liashchynskiy, P. (2019). Grid search, random search, genetic algorithm: a big comparison for NAS. *arXiv preprint arXiv:1912.06059*.
- Mahdavinejad, M. S., Rezvan, M., Barekatin, M., Adibi, P., Barnaghi, P., & Sheth, A. P. (2018). Machine learning for Internet of Things data analysis: A survey. *Digital Communications and Networks*, 4(3), 161-175.
- Mohammed, M., Khan, M. B., & Bashier, E. B. M. (2016). *Machine learning: algorithms and applications*. Crc Press.
- Montavon, G., Samek, W., & Müller, K. R. (2018). Methods for interpreting and understanding deep neural networks. *Digital signal processing*, 73, 1-15.
- Nawae, W., & Thongpull, K. (2020, October). Pmsm torque estimation based on machine learning techniques. In *2020 International Conference on Power, Energy and Innovations (ICPEI)* (pp. 137-140). IEEE.
- Nguyen, H., Vu, T., Vo, T. P., & Thai, H. T. (2021). Efficient machine learning models for prediction of concrete strengths. *Construction and Building Materials*, 266, 120950.
- Ni, R., Xu, D., Wang, G., Ding, L., Zhang, G., & Qu, L. (2014). Maximum efficiency per ampere control of permanent-magnet synchronous machines. *IEEE Transactions on Industrial Electronics*, 62(4), 2135-2143.
- Sarker, I. H., Kayes, A. S. M., Badsha, S., Alqahtani, H., Watters, P., & Ng, A. (2020). Cybersecurity data science: an overview from machine learning perspective. *Journal of Big data*, 7, 1-29.
- Sarker, I. H. (2021). Machine learning: Algorithms, real-world applications and research directions. *SN computer science*, 2(3), 160.
- Shalev-Shwartz, S., & Ben-David, S. (2014). *Understanding machine learning: From theory to algorithms*. Cambridge university press.
- Song, Y. Y., & Ying, L. U. (2015). Decision tree methods: applications for classification and prediction. *Shanghai archives of psychiatry*, 27(2), 130.
- Vishwakarma, S., Kumar, A., & Vishwakarma, A. (2022, November). Torque Estimation of Permanent Magnet Synchronous Motor (PMSM) Using 1D Convolutional Neural Network. In *2022 IEEE 6th Conference on Information and Communication Technology (CICT)* (pp. 1-5). IEEE.



Werbos, P. J. (1990). Backpropagation through time: what it does and how to do it. *Proceedings of the IEEE*, 78(10), 1550-1560.

Wu D, Jennings C, Terpenney J, Gao RX, Kumara S. A comparative study on machine learning algorithms for smart manufacturing: tool wear prediction using random forests. *J Manuf Sci Eng* 2017;139(7):1–10.

Xin, Y., Kong, L., Liu, Z., Chen, Y., Li, Y., Zhu, H., ... & Wang, C. (2018). Machine learning and deep learning methods for cybersecurity. *Ieee access*, 6, 35365-35381.

Yan, Y. B., Liang, J. N., Sun, T. F., Geng, J. P., & Pan, D. J. (2019, August). Torque estimation and control of PMSM based on deep learning. In *2019 22nd International Conference on Electrical Machines and Systems (ICEMS)* (pp. 1-6). IEEE

Zhang, A., Lipton, Z. C., Li, M., & Smola, A. J. (2021). Dive into deep learning. *arXiv preprint arXiv:2106.11342*.